Chapter 10
Magnetic Nanomedicine

M. Zubair Iqbal, Gohar Ijaz Dar, Israt Ali, and Aiguo Wu

Abstract Nanotechnology emerged as a promising field of science with a diversity of applications in energy storage, biotechnology, medicine, sensing, and healthcare monitoring and in each aspect of nature. Owing to the significant characteristics of the smaller size, easy modification, and tunable physical and chemical properties, magnetic nanomaterials have gained potential fame in the nanomedicine field. In terms of treatment and diagnosis, magnetic nanoparticles (MNP) cannot be replaced with any other material. Surface functionalization and coating of ferromagnetic and superparamagnetic nanoparticles not only make them biocompatible but also effective for drug delivery and killing tumor cells. In this book chapter, we highlighted the emerging applications of magnetic nanoparticles, from synthesis to potential applications. Specifically, brief introduction of magnetic nanomaterials and their physical properties is discussed in detail. Further, the facile synthesis methods to prepare MNPs and recent developments in MNPs as magnetic hyperthermia agents, as a drug transporter, and use in magnetic resonance imaging as a contrast agents are also elaborated profoundly.

M. Z. Iqbal
Department of Materials Science and Engineering, Zhejiang Sci-Tech University, Hangzhou, People's Republic of China

Cixi Institute of Biomedical Engineering, CAS Key Laboratory of Magnetic Materials and Devices, & Key Laboratory of Additive Manufacturing Materials of Zhejiang Province, & Division of Functional Materials and Nanodevices, Ningbo Institute of Materials Technology and Engineering, Chinese Academy of Sciences, Ningbo, People's Republic of China

G. I. Dar · A. Wu (✉)
Cixi Institute of Biomedical Engineering, CAS Key Laboratory of Magnetic Materials and Devices, & Key Laboratory of Additive Manufacturing Materials of Zhejiang Province, & Division of Functional Materials and Nanodevices, Ningbo Institute of Materials Technology and Engineering, Chinese Academy of Sciences, Ningbo, People's Republic of China
e-mail: aiguo@nimte.ac.cn

I. Ali
Division of Polymer and Composite Materials, Ningbo Institute of Material Technology and Engineering, Chinese Academy of Sciences, Ningbo, People's Republic of China

X. Xue (ed.), *Nanomedicine in Brain Diseases*,
https://doi.org/10.1007/978-981-13-8731-9_10

Keywords Nanomaterials · Magnetic nanoparticles · Magnetic hyperthermia · Drug delivery · Magnetic resonance imaging

10.1 Nanomaterials

The concept of nanotechnology is coined by Richard P. Feynman (Nobel Laureate in Physics 1965) approximately 50 years ago. The nanotechnology word was first time used during the American Physical Society (APS) annual meeting which was held at California Institute of Technology (December 1959) [1]. However, researchers have not solidly identified the specific definition of nanomaterials. Generally, scientists are agreed that nanomaterials are partially described by their minute dimensions which can be measured in nanometers [2]. A nanoscale is recognized as one millionth of a millimeter, approximately 1/8000 the diameter of a human hair. Nano-sized phenomena also exist in nature such as the size of the bacterium, virus, antibody, and DNA molecules [3]. Nanoscale materials are the base of nanoscience and nanotechnology. Nanomaterial engineering is a broad and multidisciplinary research area which has been involved rapidly into human usage to comfort their living styles. Nanomaterials have already admirable commercial impacts in the form of nanomaterial-based industrial products and will definitely increase in the future [4].

Nanomaterials can be obtained from many products, such as carbon or different natural minerals. However, nanomaterials are restricted to have at least one dimension less than 100 nm. Special high-resolution microscopes are employed to examine the structural properties of nanomaterials rather than conventional lab microscopes. Michael Faraday presented one of the earlier scientific reports on gold nanoparticles in 1857 [5]. Later, metallic nanopowders were synthesized in the 1960s and 1970s and used for magnetic recording tapes. Nanotechnology took a prosperous consideration in the twentieth century, and scientists are either producing or utilizing nanomaterials or nanomaterial-based products [6].

Figure 10.1 shows the correlation between nano-sized materials and their comparison in living beings [7]. Nanomaterials can be in the form of single, aggregated, or fused forms with spherical, irregular, and tubular shapes. However, researchers have been paying attention to prepare many beautiful structures to change in their electrical, optical, mechanical, and magnetic properties for different purposes [8, 9]. The properties of the nano-sized materials are significantly different than the bulk materials (macro and micro) owing to their large fraction of surface atoms, spatial confinement, high surface energy, and reduced imperfections. Due to these attractive properties, nanomaterials are having a broad range of applications in the field of environmental protection, electronics, energy storage, agriculture, home appliances, food industry, and medicines [10, 11].

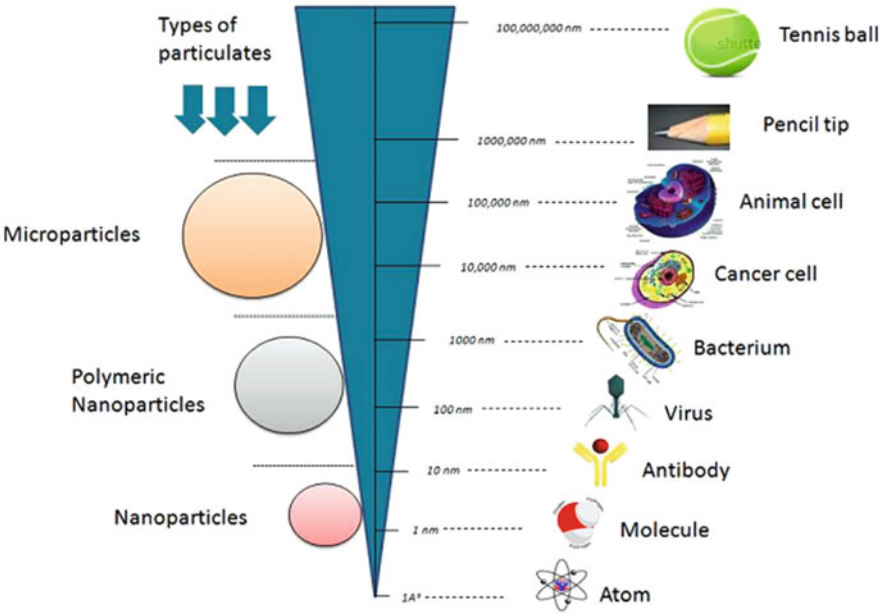

Fig. 10.1 Scale representing the size between particles and main living units. (Reprinted with permission from reference [7])

10.2 Magnetic Nanoparticles

Nanoparticles of magnetic materials have been attaining significant attraction because of their promising applications in biomedicine, gyroscopic sensors, magnetic storage, catalysis, neural stimulation, and spintronics [12, 13]. In the past two decades, MNPs having one dimension in nanoscale are the imperative class of nanomaterials which has been growing rapidly, and their realm is expanding for the science and technology. The controllable size of the MNPs presents unique qualities in nanomedicine, and their sizes are comparable biological system such as a gene (2 nm wide and 10–100 nm long), a protein (5–50 nm), a virus (20–450 nm), and a cell (10–100 μm) [14, 15]. These kinds of special features are very hard to observe in bulk materials. Bulk magnetic materials show high saturation magnetism, but they cause intense toxicity which limits their use in clinical application. However, MNPs are considered to be safe and manipulate by external magnetic field. This process is very exciting in the sense of transferring energy with the help of external magnetic field to the MNPs. By this practice, MNPs can be heated and used as hyperthermia agents and chemotherapeutic agents, transporting the attached targeting molecules to the desired place. Therefore, these special physical properties

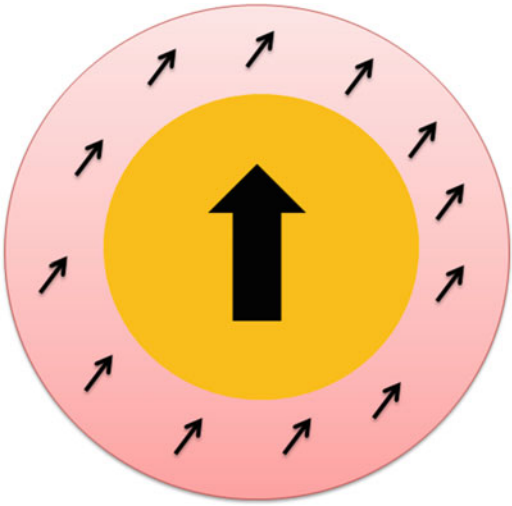

Fig. 10.2 Schematic diagram of general spin canting process

of MNPs made them promising applicants in magnetic nanomedicine [16]. The volume of the magnetic core Vm, magnetic moment, and magnetization are important factors of MNPs for magnetic nanomedicine (MNM) and associated applications. The dimensions and shapes of the MNPs are strongly related with the magnetic moment and anisotropy constant. A strong applied magnetic field is favorable for drug/gene delivery-related applications, whereas higher magnetic moment is appropriate for molecular imaging and detection [17, 18].

The number of atoms increases onto the surface of nanoparticle as the size reduces in nanometer range. As a result, magnetic characteristics at the surface vary than the inner core, disturbance of the translational crystal symmetry of the nanoparticle, which leads to increase in the anisotropy constant and decrease in the saturation magnetizations of the MNPs. This effect is called spin-canting effect, and it only influenced on the core of the MNPs but have not been affected by organic coating [19, 20]. If the nanoparticle is divided into two parts such as the core and the surface layer which is considered as the shell, then spin-canting effect can be easily understood as shown in Fig. 10.2. In the presence of external magnetic field, aligned spins are observed in the core and canting spins in the shell layer.

The saturation magnetization of the spherical MNPs can be given [21].

$$M_s = M_{sb}\left(1 - {}^{2\delta}\!/_{D}\right)^3 \tag{10.1}$$

where saturation magnetization of the MNPs is denoted by M_s, M_{sb} is the saturation magnetization of the bulk materials, δ is the thickness of the spin canting layer, and D is the diameter of the magnetic core.

The perceived anisotropy constants of MNPs are most of the time greater than their consistent bulk materials because of spin-canting effect.

$$K_{eff} = K_b + (^{6\Phi}/_{D})K_s \tag{10.2}$$

where K_b and K_s are the bulk and surface anisotropy constants, respectively [22, 23].

The effective anisotropy including shape and surface anisotropy strongly depends on the shape, and shape anisotropy is insignificant as compared to surface anisotropy for the spherical-shaped MNPs. Researchers have examined the magnetic properties of magnetic nanomaterials using diameters of magnetic core by the abovementioned two models [20].

The magnetization of magnetic materials is magnetic moment per unit volume, and the relation is given in Eq. 10.3. Magnetization and magnetic moment determine that how a nucleus responds to the external magnetic field.

$$M = mB_o \tag{10.3}$$

where B_o is the external applied magnetic field, m is the magnetic moment, and M is the magnetization.

Magnetic properties are strongly depending on the electronic structure of the material. A magnetic spin or domain (Weiss domain) refers to the dimensions of ferromagnetic material, where all magnetic dipoles have the same alignment with the exchange forces.

This concept of the materials spin or magnetic domain in the magnetic material is categorized into diamagnetic, ferromagnetic, paramagnetic, and superparamagnetic. Size-dependent magnetic behavior is also observed by domain structure of magnetic materials. The assessment of *m* for the substance is a multiplication of the magnetic moments of the atoms from the substance. Moreover, susceptibility (χ), where $\chi = M/H$, and permeability (μ), where $\mu = B/H$, are employed to measure the response of a material to magnetic field. For example, the iron atom shows high magnetic moment due to its unpaired electrons and presents different magnetic behaviors (Fig. 10.3).

Furthermore, large particles show similar behavior as bulk materials. The size-dependent magnetic properties can be observed in ferromagnetic materials. For example, at critical size Dc, the ferromagnetic material converts into a single domain. Generally, the critical size Dc is the range between 10 nm and 100 nm.

$$D_C \approx 18\frac{\sqrt{AK_{eff}}}{\mu_o M^2} \tag{10.4}$$

where K_{eff} is the anisotropy constant, A the exchange constant, and μ_0 the vacuum permeability. A single-domain particle is homogeneously magnetized and aligned parallel to the applied external magnetic field to give very high coercivity [25].

Many important parameters, such as magnetic saturation value, surface or domain wall energy, particle shape, the strength of the crystal anisotropy, and exchange forces, are influenced on the critical size of the single domain by the magnetic domain theory. Mostly materials possess magnetism in the presence of B_o. However,

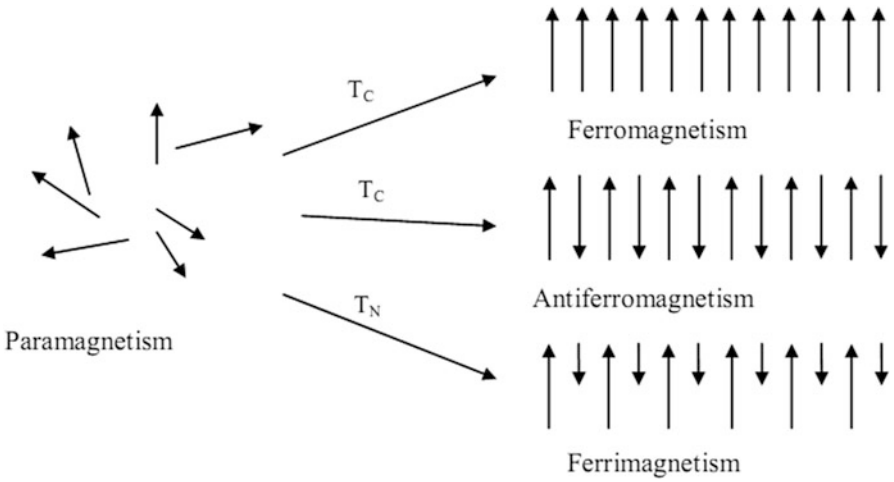

Fig. 10.3 Arrangement of single atomic magnetic moment in different kinds of magnetic materials. (Reprinted with permission from reference [24])

some materials produced strong, and some show weak, magnetic behavior. Diamagnetism is very weak because electronic subshells of diamagnetic materials are filled, and magnetic moments are paired, canceling the overall effect. In case of ferromagnetic materials, magnetic effect is not zero because of magnetic moment of unpaired electrons under the applied field, and these materials have some remanence and coercivity termed as hysteresis loop. As the coercivity is strongly related to the size of the MNPs, such as by decreasing the particle size, the value of coercivity increases to a maximum and then reduces to zero. The relation between the nanoparticle size and magnetic domain structure is shown in Fig. 10.4.

In superparamagnetism, the coercivity value becomes zero because the dimensions of single-domain particle reduced or even less than critical diameter. Kittel presented the theoretical hypothesis in 1946 about superparamagnetism and the critical size of the particle having single magnetic domain. Superparamagnetism is a process in which MNPs indicate the same behavior as paramagnetism at temperatures below the Néel or the Curie temperature. This shows that superparamagnetism behavior is induced by thermal effects. Apart from other properties, superparamagnetic nanoparticles exhibit short relaxation time which is a very promising characteristic in hyperthermia applications. Their magnetic moments are rapidly reoriented in the presence of an alternating external magnetic field and return to a nonmagnetic state after removing the external magnet source; as a result MNPs release heat to surrounding atmosphere because of fast changes in the strength and frequency of magnetic field. This special feature of manipulation of MNPs only under magnetic force makes them promising when introduced to biological environments. Ferromagnetism can be observed in various crystalline materials other than Fe, Co, or Ni. However, iron is highly magnetic and naturally available mineral.

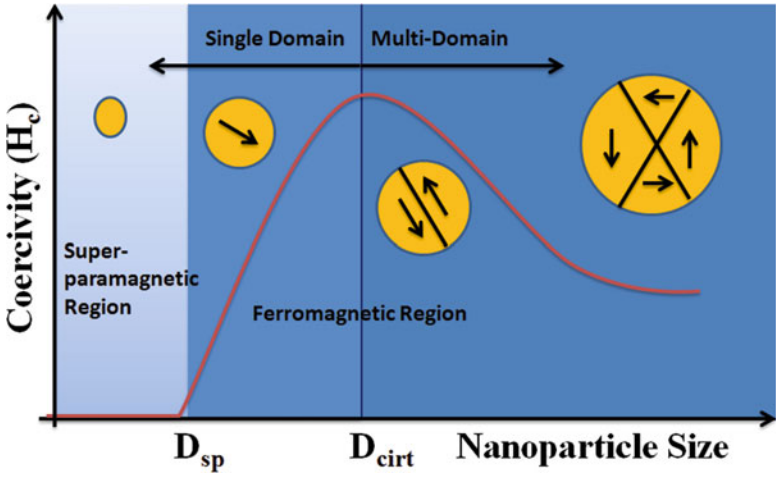

Fig. 10.4 Graphical representation of the coercivity-size relationship with respect to MNPs

Therefore, it has commonly used to prepare superparamagnetic nanoparticles which widely employed as magnetic nanomedicine agents [26–29].

10.3 Synthesis Method of MNPs

Researchers have been paying attention to develop cost-effective materials synthesis techniques to produce fine nanoparticles with enhanced properties for industrial and technological applications. Presently, various chemical and physical methods have been employed for the preparation of nanomaterials with controlled dimensions [30–33].

Generally, two basic materials synthesis methods have been used frequently, top-down and bottom-up approaches. In the top-down process, a synthesis route starts from a large piece of particles and consequently reduces the size to create small particles (nanoparticles). Top-down process includes ball milling and bulk materials (or thin films). Alternatively, bottom-up technique uses self-assembly growth process on minute components of atomic or molecular dimensions to organize them into nanoparticles by using external force or natural physical principle [34, 35]. The schematic illustration of these two methodologies is shown in Fig. 10.5.

Both methods have benefits and limitations related to fast synthesis, reproducibility, cost, and easy and complicated handling. Frequently, monodisperse MNPs can be prepared by various chemical methods. In the last two decades, plentiful research has been carried out on the preparation of MNPs. MNPs have been prepared with various shapes, dimensions, and phases. These MNPs included magnetic alloys such as $CoPt_3$ and FePt [37, 38]; spinel-type ferromagnets such as $MgFe_2O_4$,

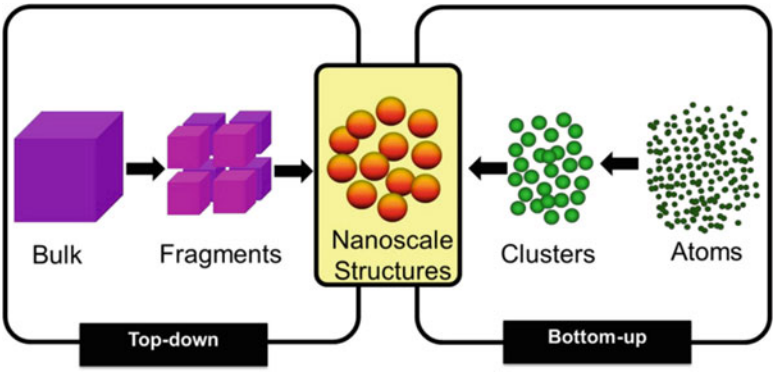

Fig. 10.5 Schematic illustration of the formation of nanostructures via the top-down and bottom-up approaches. (Reprinted with permission from reference [36])

$MnFe_2O_4$, and $CoFe_2O_4$ [39, 40]; iron oxides such as Fe_3O_4 and γ-Fe_2O_3 [41]; and pure metals such as Fe and Co [42, 43]. The following section will describe some interesting and useful physical and chemical synthesis techniques for the fabrication of fine monodispersed MNPs.

10.3.1 Ball Milling Method

The basic physical method in top-down approach is ball milling method which was developed by John Benjamin in 1970. In this technique, a sample is grounded to prepare the reduced size nanopowder [44]. This is a very promising technique among other physical methods to prepare the MNPs. Basically, there are three steps involved to fabricate the nanoparticles in ball milling method. Firstly, mechanical energy is delivered by balls to bulk materials and then collisions occurred between balls and bulk substance. The disruption density remains increasing with milling time. Due to this high energy transformation, physical and chemical properties of the materials change. Secondly, small particles are produced by rearrangement of dislocations. Finally, orientation of the grain became random, and small particles get rid from large materials. In case of MNPs, a magnet placed outside the tube which attracts the peeled of nanoparticles. Ball milling equipment is easy to handle but has long production cycle [45, 46]. However, there are some limitations associated with this method, such as contamination problems, polydisperse size distribution, and partially amorphous state. Also, the aggregation of particles is observed if the ball milling time increases, and likewise aggregation happens in small particles to reduce surface energy [47, 48].

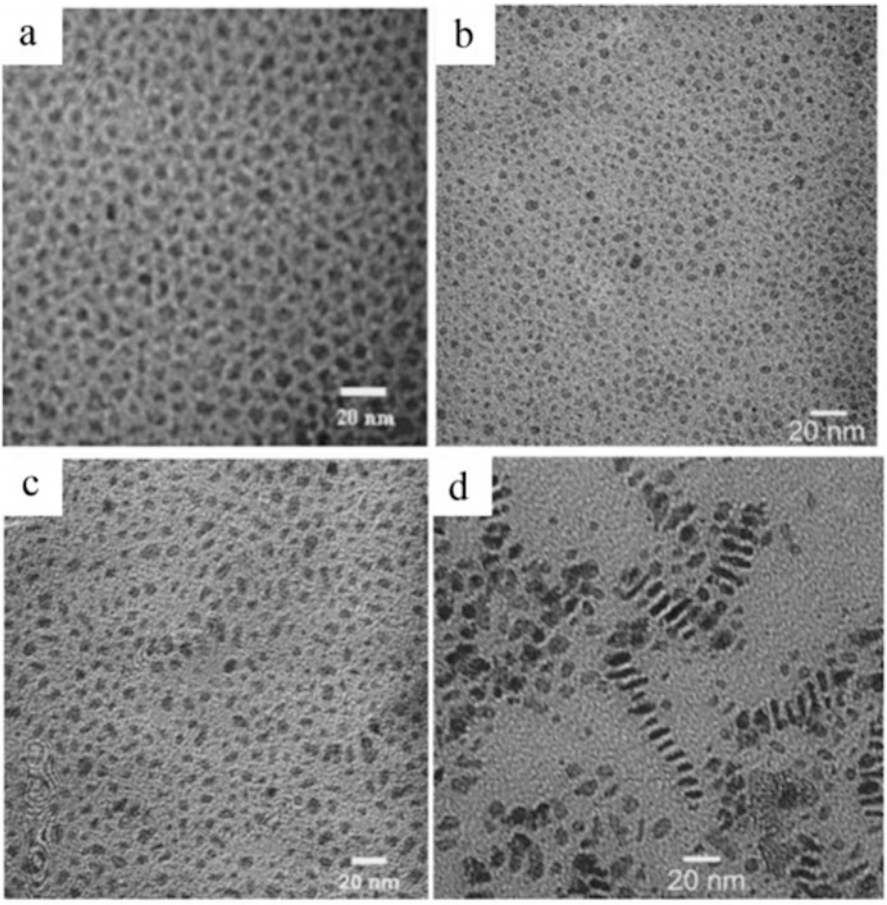

Fig. 10.6 Transmission electron microscope images of the synthesized MNPs by ball milling method at different time. (Reprinted with permission from reference [49])

Researchers have been focusing on how to produce homogeneous size distribution of MNPs by using ball milling procedure. Some reports proposed the centrifugal separation method with different centrifuge speeds to collect different sizes of the NPs. In this way, magnetic nanoparticles and their composites are synthesized with narrower size distributions [50]. TEM pictures of Fe and $SmCo_5$ NPs synthesized by this method are shown in Fig. 10.6. 4–6 nm of Fe NPs and 3–13 nm of $SmCo_5$ NPs are obtained and shown in Fig. 10.6 (a, b). Also, Fig. 10.6 (c, d) shows the TEM images of $SnCo_5$ NPs at several milling times. Fe, Co, and FeCo NPs were fabricated by surfactant-assisted ball milling method. By controlling the parameters of ball milling equipment and applying size selection process, homogeneous sized 6 nm MNPs are obtained.

10.3.2 Chemical Methods

It is obvious that small NPs have high surface to volume ratio. Therefore, they agglomerate easily to reduce their surface energy. In case of superparamagnetic MNPs, aggregation effects are very high because of their colloidal nature. Fabrication of monodispersed MNPs is a complex process, and this is still a challenging task to synthesize MNPs with controlled size and reproducible at large scale without any difficult purification procedure. Various chemical routes can be utilized to prepare the magnetic nanoparticles for biomedical application such as sonochemical reactions [51], sol-gel method [52], microemulsion [53], flow injection synthesis [54], electrospray synthesis [55], electrospray synthesis [56], hydrothermal reactions [57], and thermal decomposition method [58]. While due to the colloidal complexion, the preparation of superparamagnetic nanoparticles is a little bit complicated process. Different methods have been utilized to synthesized magnetic nanoparticles with various phases and compositions, including pure metals like Co and Fe [59], iron oxides like Fe_3O_4 and Fe_2O_3, alloys such as FePt and CoPt [37, 60], as well as spinel-type ferromagnetic materials such as $MgFe_2O_4$ and $CoFe_2O_4$ [39, 61]. In the last few years, numerous efforts have been dedicated for the preparation of MNPs with control morphology, well stable and monodisperse through various chemical routes such as thermal decomposition, hydrothermal reactions, coprecipitation method, and laser pyrolysis techniques. Among them, the thermal decomposition method and hydrothermal reaction are extensively utilized to fabricate the MNPs with narrow size distribution and homogeneous composition. Here we attempt to sum up some discussion about the coprecipitation, thermal decomposition, and hydrothermal methods for the preparation of magnetic nanoparticles with an illustration of some examples.

10.3.3 Coprecipitation

The coprecipitation technique is very promising and efficient chemical method to prepare the MNPs especially superparamagnetic NPs. The biodegradable MNPs can be synthesized at large scale and highly aqueous dispersed by using this method. MNPs with different sizes, structures, and compositions can be obtained, but these properties depend on the initial magnetic salt precursor types, reducing agents, reaction time, and temperature. Once the optimized synthesis conditions are achieved, MNPs are reproducible by coprecipitation technique.

In case of iron oxide NPs, ferrous and ferric salts are mixed to prepare MNPs by an aging stoichiometric in aqueous medium. The chemical reaction involved in the synthesis of Fe_3O_4 NPs is given in Eq. 10.4.

$$M^{2+} + 2Fe^{3+} + 8OH^- \rightarrow MFe_2O_4 + 4H_2O \tag{10.5}$$

where M can be Fe^{2+}, Mn^{2+}, Co^{2+}, Cu^{2+}, Mg^{2+}, Zn^{2+} and Ni^{2+}.

With a stoichiometric ratio of Fe^{3+} and M^{2+} is 2:1, the complete precipitation should be obtained at a pH levels between 8 and 14 in nonoxidizing atmosphere [62].

Fe_3O_4 is unstable at some circumstances and are easily oxidized to maghemite (γ-Fe_2O_3) in the presence of oxygen.

$$Fe_3O_4 + 2H^+ \rightarrow \gamma Fe_2O_3 + H_2O \tag{10.6}$$

Many other factors are also related to the oxidation of iron oxide apart from the air.

However, in the formation of MNPs, particularly Fe_3O_4 by coprecipitation method, there is still challengeable that how to obtain the narrow size distribution with controlled size and shape. Shen et al. prepared ultrasmall nanoparticles of iron oxide using coprecipitation and successfully applied in biomedical application [63]. Michael Barrow et al. also synthesized superparamagnetic iron oxide nanoparticles with different sizes by coprecipitation approach [64].

10.3.4 Thermal Decomposition

The considerable issue is to prepare the extremely fine particles with control size and distribution at nanoscale formulation. This problem is prominent when dealing with MNPs because of their continual growth with reduction of altogether surface energy as well as aggregation of particles. Furthermore, the *Ms* value is being significantly decreased than bulk materials at nanoscale systems [65–68]. While the preparation of MNPs with control size and homogeneous size distribution as well as with less *Ms* value is potentially important in the biomedical field, the thermal decomposition is a promising method to synthesize magnetic nanoparticles with the decomposition of organometallic compounds comprised of stabilizing surfactants and organic solvents without aggregation of particles [39, 69–71]. After the successful synthesis of various oxides and high conductive semiconductor nanocrystal through thermal decomposition [72, 73], corresponding method has been forward to the synthesis of MNPs with control and homogeneous morphology distribution. While the magnetic nanocrystals have been fabricated via thermal decomposition method by using organometallic compounds with high-boiling solvents including stabilizing surfactants [74], further, the metal acetylacetonates included in the organometallic precursors such as metal cupferronates [M^xCup_x] (M = metal ion; Cup = N-nitrosophenylamine, $C_6H_5N(NO)O$-) [75] [M(acac)n] (M = Mn, Fe, Ni, Cr, Co, n = 2 or 3, acac = acetylacetonate), oleic acid [76], hexadecylamine [77], and fatty acids [78] are frequently used as surfactants. Accordingly, the ratios of reagents, reaction time, and temperature, as well as aging period, are the determined parameters toward synthesizing of magnetic nanoparticles with tunable size having homogeneous morphological distribution. In the case of zerovalent metal in the precursor like in carbonyls, initially the formation of metal is being carried out through thermal decomposition, but oxide nanoparticles as well can be synthesized by a two-step procedure. Meanwhile, the precursors include cationic metal centers, the process of

thermal decomposition directly produced the Fe_3O_4 NPs by decomposition of $[Fe_2(acac)_3]$ in the presence of various hydrophobic materials [79]. Peng et al. prepared manganese-based nanocrystals with controlled shapes and size using thermal decomposition method [78]. Maity and co-workers reported the synthesis of MNPs of iron oxide using acetylacetonate $[Fe(acac)_3]$ through thermal decomposition and studied the various effects on the structure of the Fe_3O_4 nanoparticles [80]. The particle size was well controlled with narrow size distribution, and *Ms* value is significantly enhanced with increasing the temperature and reaction time. Further, in this work saturation magnetization Ms. value of particles can be raised up through long reaction time or high reaction temperature, if the particle size can be conserved through either by usage of solvent-free thermal decomposition process or adhesion of oleic acid to the particle surface. The development performance and nucleation of nanoparticles formulations can be qualitatively illuminated by classical concepts. Ostwald ripening [81] and LaMer supersaturation [82] processes describe what is complied, specifically in the kinetically controlled synthetic procedures. Like other magnetic nanoparticles, superparamagnetic iron oxide (SPION) nanoparticles are synthesized by thermal decomposition methods with controlled sized distribution which are further suitable for numerous biomedical applications such as imaging [83], diagnostics [84], and targeting therapy [85]; SPIONs are considered to be nontoxic for intravenous investigations [86, 87]. Hufschmid et al. prepared the SPIONs with good dispersion by thermal decomposition approach and compared the three common iron-containing precursors such as iron(III) oleate (Fe $[C_{18}H_{33}O_2]_3$), iron pentacarbonyl ($Fe[CO]_5$), and iron oxyhydroxide (FEOOH) [88]. In this work, by using organic solvents, iron oxide particles were grown by thermal decomposition, and through generally excess surfactant, oleic acid is added to adjust size distribution and tailor the growth kinetics. By the addition of more oleic acid, the size of particles was altered from 10 to 25 nm and the quantity of oleic acid increased, resulting in increased sizes of particles. In another work, Iqbal et al. synthesized the ultrasmall silica-coated SPIONs by thermal decomposition of iron oleate complex with an average size of 4 nm with homogeneous size and monodispersion [89]. In this synthesis process, iron oleate was used as a precursor in the presence of organic solvents oleic acid and oleyl alcohol. The solution reaction color with respect to time and microscopic images of prepared SPIONs is shown in Fig. 10.7.

Characterization techniques revealed the good crystallinity and high dispersion of MNPs in organic and aqueous solution. Further, these nanoparticles are utilized as an excellent candidate for MRI imaging as T_1 contrast agent due to their smaller size and homogeneous distribution. Moreover, various pure composites of MNPs can be prepared by the thermal decomposition approach [90–93].

10.3.5 Hydrothermal Synthesis

There is a broad range of nanomaterials including magnetic nanoparticles that have been synthesized through the hydrothermal approach. To prepare ultrafine

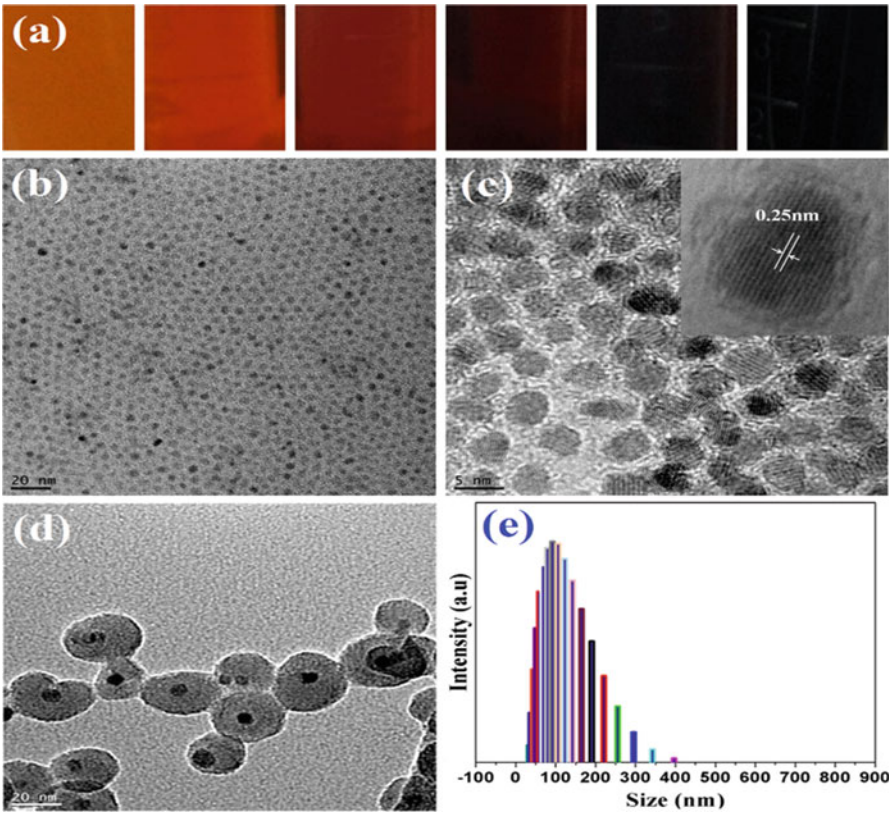

Fig. 10.7 (**a**) Digital snapshots of solution reaction color with respect to time (**b**-**d**) TEM images of the ultrasmall nanoparticles and the SiO_2-coated Fe_3O_4 nanoparticles. (**e**) Particles size dispersion analyses of Fe_3O_4@SiO_2 in water. (Reprinted with permission from reference [89])

nanopowders and MNPs through hydrothermal reactions is widely reported in literature [93–95]. In the hydrothermal approach, the reactions take place in aqueous media in autoclaves or reactors where the temperature is more than 200 °C and pressure might be higher than 2000 psi. Li et al. described the typical synthesis route of hydrothermal reaction from a broad diversity of nanocrystals which has been synthesized through liquid-solid solution reaction [96]. The approach comprised of a water-ethanol solution, a metal linoleate (solid), and an ethanol-acid liquid phase under a hydrothermal atmosphere at various reaction temperatures. The fundamental point in this mechanism is phase transfer and separation strategy which happens at the interfaces of solid, liquid, and solution phases immediate throughout the synthesis. Generally, two mechanisms are defined for fabrication of ferrites through hydrothermal conditions, oxidation or nucleation and hydrolysis of hybrid metal hydroxides. There is quite a similarity that exists between these two mechanisms except the usage of ferrous salts in the second mechanism. In this approach, significantly effects are being occurred on resultant products by reaction conditions such as time and temperature of reaction and solvents [97]. Undeniably, it is

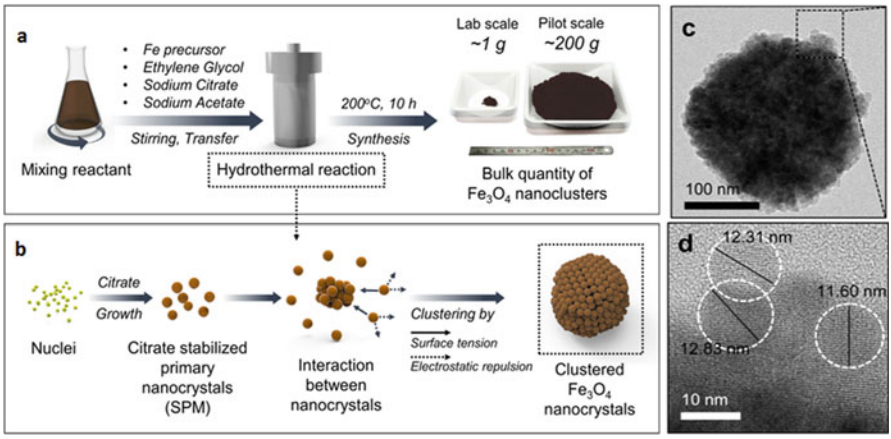

Fig. 10.8 (**a**–**b**) Schematic presentation of the procedure for the gram-scale synthesis of MNCs. (**c** and **d**) A set of transmission electron microscopy (TEM) images of MNCs. (Reprinted with permission from reference [107])

observed that the precipitation of larger Fe_3O_4 nanoparticles resulted due to higher water content and the particle size increased due to prolonged reaction time. In the hydrothermal approach, the grain growth and the nucleation process rate mainly control the particle size in crystallization. By keeping other conditions unchanged, their process rate is determined by reaction temperature [97]. The solvo−/hydrothermal approach provides a cost-effective and versatile route for the fabrication of a large number of magnetic clusters with high crystallinity and controlled morphology [98, 99]. The hydrothermal approach is capable to prepare and reshape the nanoparticles via different processes to modify the magnetic behavior of resultant particles [100]. Recently, Kim et al. reported the gram scalable synthesis of superparamagnetic iron oxide nanoclusters Fe_3O_4(MNCs) of 11–13 nm composed of nanocrystals by the hydrothermal approach and modify the MNCs morphology by the diversity of molar ratios of surfactants and precursors [101]. The schematic presentation of the process of the preparation of Fe_3O_4 nanocluster is shown in Fig. 10.8. Usually, the ferrite substances might be categorized into three classes: garnet ferrites, hexagonal ferrites, and spinel ferrites [102–104]. In another work, Hedayati and co-workers reported the fabrication of Fe_3O_4 nanoparticles through hydrothermal synthesis and then investigated the magnetic properties [105]. Further, the outcome of the resultant morphology was investigated due to different surfactants such as cationic and anionic. Li et al. reported the synthesis of nanocomposites of α-Fe_2O_3/rGO through a simple hydrothermal approach with the observation of photocatalytic performance and negative MR effect [106].

In the preparation mechanism of MNPs through different approaches, the colloidal stability results from either electrostatic or steric repulsion, based on the polarity of the solvent and stabilizers such as amines or fatty acids used. Although the nanoparticles prepared through thermal decomposition are usually satirically stabilized by surfactants or fatty acids in an organic solvent [71].

10.4 Magnetic Nanoparticles as Hyperthermia Agent

Nanotechnology emerged as a prodigious field of science with a diversity of applications in biotechnology, medicine, sensing, and healthcare monitoring and in each and every aspect of nature [108–110]. Due to the smaller size, easy modification, and tunable physical and chemical properties, nano-sized materials have gained potential fame in the nanomedicine field [111–113]. In terms of treatment and diagnosis, magnetic nanoparticles (MNP) cannot be replaced with any other material [25, 114, 115]. Surface functionalization and coating of ferromagnetic and superparamagnetic nanoparticles not only make them biocompatible but also effective for killing tumor cells [116, 117]. By applying an alternative field, activation of MNP brings targeted therapeutic heating of tumor. Gilchrist et al. have explained firstly that by administration of B_o, the lymphatic metastases can be killed effectively due to the heating mechanism in 1951 [118]. Heating of MNPs by applying an external B_o to induce killing of a tumor cell is a well-known term for magnetic hyperthermia [119]. According to Néel or Brown relaxation due to hysteresis losses, thermal energy is released into the environment [120, 121]. Basically, hysteresis loss is related to the nature and strength of applied external B_o which further induced the increase in hyperthermia effect. Originally, various sizes of MNPs endure the applied external B_o; the alignment of MNPs against or with the direction of the applied magnetic field happens. The time delay phenomenon between the reverting back to normal state and magnetizable causes the generation of Brownian relaxation [122, 123]. The movement of these aligned states of nanoparticles and friction between them generates heat in the surrounding. This heat is used to kill or prolong the growth of tumor. So, to induce the magnetic hyperthermia, Brownian relaxation and generation of heat are the key parameters. In the past, there were different kinds of mechanisms that are involved to cure cancer like radiation therapy, chemotherapy, and surgery [124–126]. As all the therapeutic mechanisms have some drawbacks like cisplatin which is widely used to cure cancer but is harmful for the bone marrow, by combining different therapy mechanisms, therapeutic index can be improved [127]. In combination with other traditional cancer therapies, hyperthermia has shown promising effects without damaging other healthy tissues. Hyperthermia has been revealed promising not only as a singular therapy but also in conjunction with traditional cancer treatments such as chemotherapy and radiation. Since the quantity of heat produced can be observed during local hyperthermia, harm to nearby tissue can be evaded or minimized. Pain, discomfort, and burns are the most common effects that can be caused by hyperthermia [128, 129].

Fe, Fe_3O_4, Ni, strontium ferrite, and chromium oxide have been used extensively to produce MNPs [130]. The Curie temperature value along with other physical properties of such kind of materials containing a core of magnetic nanoparticles has shown great compatibility in animal studies. In terms of magnetic nanoparticles, iron oxide (Fe_3O_4) nanoparticles and their core-shell structures have gained fame in the nanomedicine field [131, 132]. There are different advantages of Fe_3O_4 nanoparticles over other magnetic nanoparticles; the most important one is biocompatibility and nontoxicity. Further, diversity of available synthetic procedure and

ease in functionalization of iron oxide nanoparticles with organic and inorganic biocompatible chemicals make them perfect candidates for in vivo studies and biomedical applications [133]. Similarly, cobalt ferrite has also shown high magnetization along with constant heating effect [134]. The heating efficiency of cobalt ferrite predicted to be higher than iron oxide nanoparticles as they have not studied to large extent in comparison with iron oxide nanoparticles. Despite good heating efficiencies, cobalt and nickel nanomaterials have not been studied extensively for hyperthermia or some other biomedical applications because of difficulty in synthetic procedure [135, 136]. Along with it other types of magnetic nanoparticles in the form of nanocomposite have been utilized widely for magnetic hyperthermia therapy like γFe_2O_3, $NiFe_2O_4$, $MnFe_2O_4$, $CoFe_2O_4$, NiO, and Co_3O_4 [137]. Last but not the least, gold, silver, and copper nanomaterials with wide size range and multiplicity in structure have captured the attention of researchers and proved as new comers for nanoparticles' hyperthermia [128, 138].

10.4.1 Parameters Affecting the Heating Efficiency

There are several factors influenced on the heating efficiency as discussed previous. The strength of external magnetic field plays a significant characteristic in magnetic hyperthermia, and the heating capacity of the MNPs also related to it. Generally, the external magnetic field intensity has direct relation with the power loss in magnetic hyperthermia as given in Eq. 10.7 [139]. The specific absorption rate normally increases with increasing the power of applied magnetic field [140]. Brezovich et al. observed that the product of an external applied magnetic field strength H and frequency f restricted to the value $H_f < 4.85 \times 108\ Am^{-1}\ s^{-1}$ which is not enough to provide excessive heating in patients [141].

$$P = 1/2\omega\mu 0\chi 0H2 * \omega\tau/1 + \omega 2\tau 2 \tag{10.7}$$

Nanoparticle diameter and anisotropy are also well concerned for the hyperthermia. The size of the particle is the major factor to determine that either Brownian-Néel relaxation is going to occur or hysteresis loss will cause the heat generation. In this regard, C. L. Dennis et al. studied extensively the particle size and hyperthermia effects generated by larger particle size [142]. As the particle size will be greater than 100 nm, it will not be suitable for biomedical application due to difficulty in excretion of a particle through the body, and it cannot disperse and penetrate well in the tumor. Hence, particle size should be smaller to about 15 nm which is a suitable size for the Brownian and Néel relaxation (for Fe_3O_4 nanoparticles). Heat generation below 15 nm size is due to Néel relaxation as explained in Fig. 10.9 [135].

The inferior plot demonstrates Brownian, Néel, and effective relaxation times for particles with anisotropy constants of K = 40, 25, and 10 kJ/m^3. To some extent, increasing particle concentration also affects the hyperthermia. High concentration

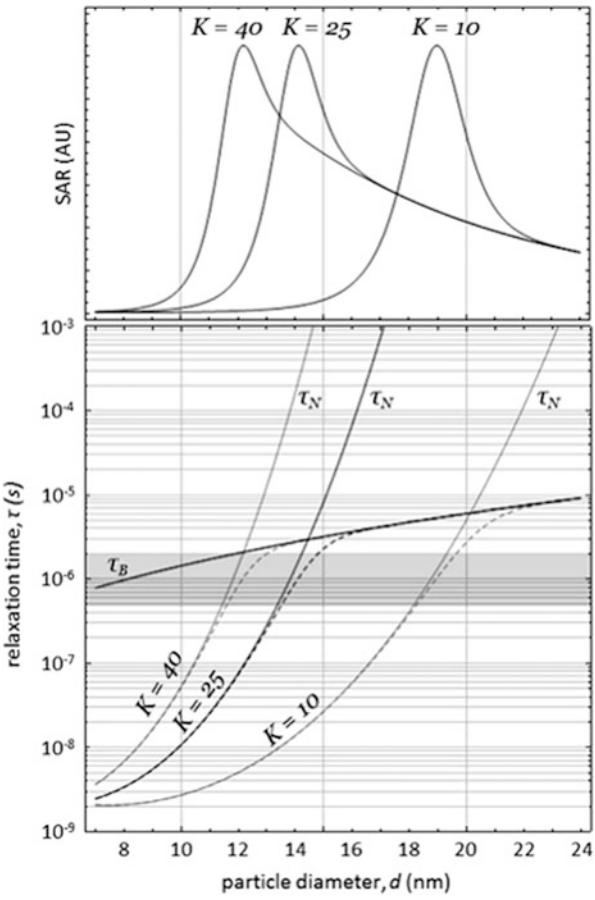

Fig. 10.9 Effect of anisotropy on relaxation time and specific absorption rate. (Reprinted with permission from reference [135])

of particles causes agglomeration and aggregation which results in higher interaction between the nanoparticles and is rarely significant for hyperthermia, while lower concentration of particles causes homogeneous distribution of nanoparticles in the fluid and significantly influences the surface absorption rate [135].

Although diversity in the synthesis of MNPs for hyperthermia can be seen from 1951 onward, as mentioned earlier iron oxide NPs are used widely. In this regard, C. L. Dennis et al. synthesized ionized ferrite nanoparticles that are core-shell structures containing Fe_3O_4 and dextran by using high-pressure homogenization method conjugated with monoclonal antibodies and have shown good results by controlling tumor growth control in a mouse after applying H = 43.8 kA m^{-1} at 150 kHz and 100% duty for 20 min [142].

In another aspect, Ching Jen Chen et al. showed that metal alloys can also be used for hyperthermia [143]. They have designed polyethylene glycol-coated magnetic Cu-Ni alloy material by polyol reduction method, and the Curie temperature measured for such an alloy system was about 43–46 °C. The material was very suitable

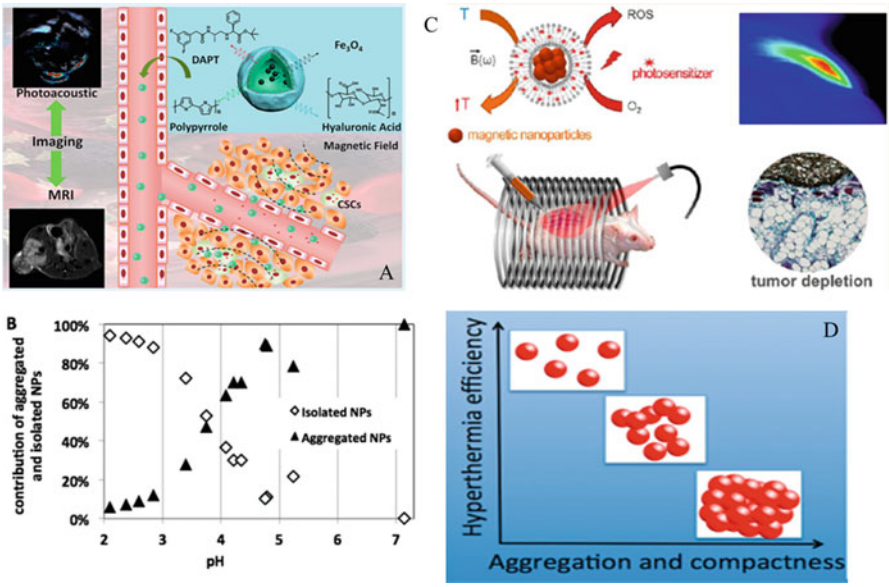

Fig. 10.10 (**a**) Photoacoustic and magnetic resonance imaging of hyaluronic acid-containing magnetic nanoparticles, (**b**) effect of pH on the aggregation of PAA-coated iron oxide nanoparticles, (**c**) photodynamic therapy and hyperthermia studies of bilayer liposomal MNPs for drug delivery and hyperthermia therapy, and (**d**) decrease in hyperthermia efficiency due to increase in aggregation of nanoparticles. (Reprinted with permission from reference [155])

for the hyperthermia to cure cancer. To achieve dual therapeutic response from a single material has become an important need due to toxicity, less availability, and desire for new materials. Recently, to realize multi-functionalities from the iron oxide nanoparticles, Claire Wilhelm et al. designed iron oxide nanocubes for magnetic and photothermal therapy [128]. They have tested three types of cancer cells (SKOV3, A431, and PC3) and successfully achieved cell death due to high heating powers to about (specific loss powers SLP) 5000 W/g. The only dual action of nanocubes can cause cell death; only hyperthermia or photothermal effect alone just inhibits the growth of tumor cell (Fig. 10.10a). In vivo study has revealed that by using dual response, the heating capacity will be higher which will inhibit the growth of tumor to a high extent (Fig. 10.10c). For comparison between spherical and cubic nanoparticles' heating efficiency, H. Srikanth et al. have studied the FeO/Fe_3O_4 nanoparticles (20 nm) [144]. By changing the ratio of FeO/Fe_3O_4, they have changed the heating efficiency for hyperthermia. Their study revealed that although spherical nanoparticles have shown higher saturation magnetization, hyperthermia experiments have shown higher values for the cubic structures. Different target molecules or polymers have been used for the hyperthermia to get accurate targeting by avoiding the other tissues loss. In this regard, Y.Q. Wang et al. have synthesized folic acid-containing magnetic nanoparticles [145]. Folic acid served as an accurate targeting agent, that is, on combination with Fe_3O_4, can provide high saturation

magnetization and fast magneto-temperature response that is necessary for hyperthermia therapy. Heat produced from such a material was recorded, and it reached up to 52.7 °F, i.e., enough to kill the tumor cell. By utilizing the magnetic response, they have studied the T_2 signal of KB cells by MRI and obtained promising results. Further after injecting the folic acid-containing magnetic nanoparticles in the mouse for KB cells, in just 4 h, the weakening of KB cells happens which was a good evidence of hyperthermia.

Recently, photothermal therapy by using some magnetic nanoparticles becomes promising therapeutic approach to cure different kinds of cancer [146]. Photothermal properties induced by black TiO_2 and other material have been used for cancer cure due to in situ heat generation [147]. Various efforts have been adopted to enhance the heating efficiency by designing new materials. Aiguo Wu et al. have synthesized poly (ethylene glycol)-modified iron oxide containing nanoflowers [148]. The in vivo and in vitro studies have shown promising results for photothermal therapy. As explained earlier the cube-shaped iron oxide nanoparticles have shown high heating efficiency, but the heating efficiency of synthesized iron oxide nanoflowers was proved to be better than iron oxide nanoparticles. Iron oxide nanoflowers have shown approximately 52 °C increase in temperature which was comparable to that of black TiO_2 core-shell nanostructures which revolutionized the biomedical field in both aspects of new nanomaterials synthesis and their advanced applications [149, 150]. To some extent, different kinds of core-shell nanomaterials have been synthesized yet for cancer, MRI, detection of various diseases, and other multifunctional tasks [151]. In this aspect to achieve application related to hyperthermia and killing cancer stem cell, Chunying Chen et al. synthesize hybrid magnetic nanomaterial for the chemo- and magnetohyperthermia therapy [152]. Hyaluronic acid was utilized to get an accumulation of this hybrid material containing Fe@PPA@HA. The use of PPr causes the photoacoustic effect, and Fe_3O_4 NPs used as MRI agent further PPr shell allowed a high amount of drug N-[N-(3,5-difluorophenacetyl-L-alanyl)]-S-phenylglycinet-butyles-ter (DAPT) loading (Fig. 10.10a). The accumulation of Fe@PPr@HA in the tumor cell and then easy drug release along with magnetic hyperthermia properties caused killing of cancer stem cells. The intraparticle interactions have been studied well by changing pH and ionic strength of the desired nanoparticles system. Poly(acrylic acid)-coated nanoparticles have shown good stability to a wide range of change of ionic strength induced by using different concentrations of ammonium chloride. For in vivo system, particle stability is a great factor to be considered. Similarly, pH variation also induced aggregation of bare and coated magnetic nanoparticles as can be seen in Fig. 10.10b. Interestingly vast variety of work has explained about multifunctionality of different materials in which utilization of properties of every material brought together in the form of one hybrid material. Claire Wilhelm et al. have designed a novel approach to utilize liposome property of hydrophilic and hydrophobic molecule transfer due to the lipid bilayer and magnetic property of magnetic (Fe_3O_4) nanoparticles [153]. The liposome has shown the photosensitizer action which on irradiation with NIR induced toxic reactive oxygen species that can induce photodynamic effect and application of magnetic field generated heating of magnetic

nanoparticles to obtain magnetic hyperthermia. Both these effects have killed the tumor that has been studied experimentally by in vitro studies (Fig. 10.10c). Regardless of the work published on the magnetic nanoparticles for the biological system, the stability mechanism is still under consideration related to the biomedical application. Well-dispersed magnetic nanoparticles have gained fame in this field, but still heating efficiency is poorly understood [154]. For the aggregation system of magnetic nanoparticles, Jerôme Fresnais et al. have explained about poly(acrylic acid)-coated and poly(acrylic acid-co-maleic acid)-coated iron oxide nanoparticles [155]. Finally, they have concluded that aggregation of magnetic nanoparticles causes decrease in heating efficiency (Fig. 10.10d).

Magnetic hyperthermia for cancer cure is not only limited to iron oxide nanoparticles, but other parameters are also involved that cause controlled hyperthermia. Orestis Kalogirou et al. have synthesized carbon-based MNPs by solvothermal method with the size range from 150 to 250 nm [156]. The heating efficiency was controlled by synthesizing thinner layer of carbon which interestingly causes the increase in specific power loss and proved efficient for hyperthermia [157]. In an instant, ultrasmall iron oxide NPs may be excreted rapidly, and biodegradation may occur on direct exposure to the biological environment [158]. To cover this limitation, a coating of a suitable material is required. Ewa Borowiak-Palen et al. have designed a sol-gel approach to get magnetic silica nanotubes (Fig. 10.11a–e) [159]. These Fe_2O_3-containing silica nanotubes were not only successfully utilized for rhodamine B drug loading but also have been

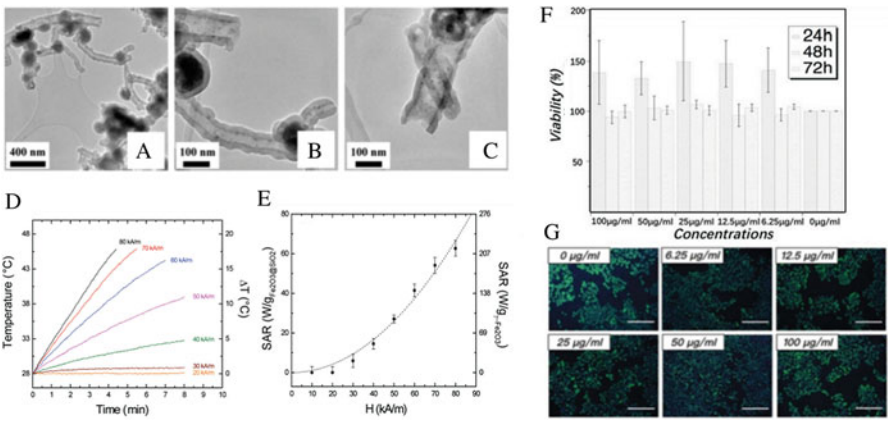

Fig. 10.11 (**a–c**) Synthesized magnetic silica nanotubes, (**d–e**) their increase in temperature according to application of various strengths of magnetic field (20 KA/m to 80 KA/m), (**f**) cell toxicity results measured by CCK-8 assay with different concentration of MNPs, and (**g**) fluorescent microscope images of separated HaCaT cells stained with various dyes. (Reprinted with permission from reference [161])

used for hyperthermia application after applying different field strengths. Further, the increase in surface absorption rate was also measured with an increase in an applied B_o for the successful elaboration of magnetic hyperthermia application. Similar to silica, carbon nanotubes have been efficiently used for hyperthermia application with other magnetic nanoparticles like Zr, Ni, Co, etc [160]. Wei Gao et al. have designed multiple magnetic nanoparticles containing carbon nanotubes ($Zn_{0.54}Co_{0.46}Cr_{0.6}Fe_{1.4}O_4$) and have determined their cytotoxicity, magnetic properties, and heat generation ability [161]. Finally, on the application of external magnetic field (frequency, 100 kHz; intensity, 200 Oe), the heat generation reached to about 42 °C which is a feasible temperature to achieve hyperthermia application (Fig. 10.11f–g). The cytotoxicity effect of magnetic carbon nanotubes was measured on HaCaT cell line by the incubation of prepared MNPs with different concentrations and time. In Fig. 10.11g, it can be seen that cells incubated with various concentrations of magnetic carbon nanotubes for 72 h have shown Calcein-positive, Hochest 33,258-positive, and PI-negative state. This toxicity result is consistent with the quantitative CCK-8 assay in Fig. 10.11f. These outcomes have revealed that the prepared magnetic carbon nanotubes demonstrated very minute level of toxicity for HaCaT cells.

The above reports showed the promising use of MNPs as a magnetic hyperthermia agent with enhanced biocompatibility.

10.5 Magnetic Nanoparticles for Drug Delivery

The treatments of fatal diseases with high efficiency have been the substantial aim of the human race since the ancient times. With passage of time, scientists have effectively refined the understanding toward the functions of human organs (bones, blood vessels, various tissues, and nerves) and other related parts including living cells with their basic phenomenon. From the last two decades, there were some incredible innovations appeared in biomedical field with polymer and micro-nanoparticles related to different ways of treatments including diagnosis, sensing, drug delivery, and imaging techniques with different therapies. Among them, drug delivery mechanism has been greatly explored to cure some fatal disease with low toxic side effects and in other clinical trials. Various species of drug carriers have been reported for different treatments including polymeric nanoparticles, micelle-shaped polymeric nanoparticles, liposomes, carbon-based systems, silica nanoparticles, and magnetic nanoparticles (e.g., iron oxides) (Fig. 10.12). Here, we discuss some magnetic nanoparticles which are used for drug delivery systems for various clinical trials. Magnetic nanoparticles are used for drug delivery system because of their control mechanism with magnetic field to cure effective part of body. In the early 1970s, the concept of using magnetic micro- and nanoparticles for drug carriers was introduced to target a specific part inside the body [162].

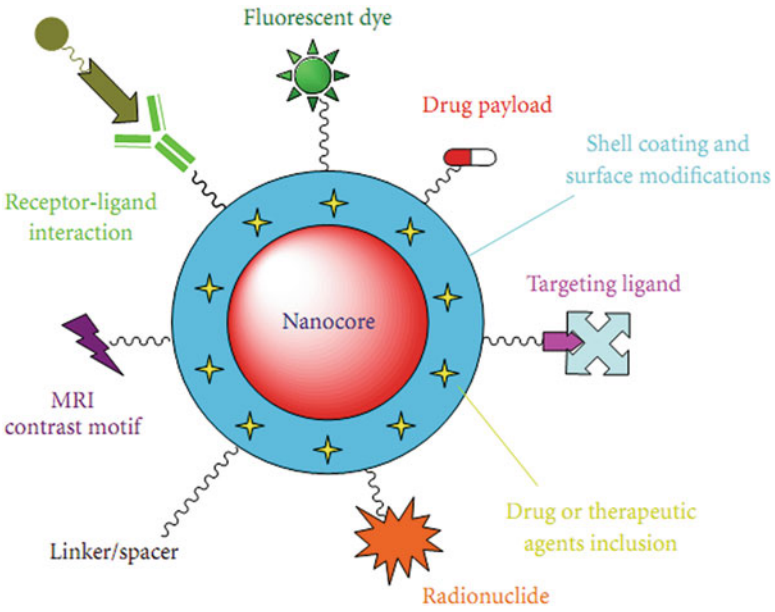

Fig. 10.12 An overview of various drug delivery systems using nanoparticles with many targeting possibilities. (Reprinted with permission from reference [163])

10.5.1 Drug Delivery Mechanism

Several drug delivery systems are being applied successfully for treatments, however still need to develop some accurate methods to overcome certain challenges that need to negotiate with development of advanced technology as well as for achieving targeted delivery of drugs. Recently, enormous progress has been devoted to hand over natural active compounds or therapeutic agents in the field of drug delivery system for various targeted treatments [164, 165]. Recently, drug delivery system based on nanotechnology studied widely that will make ease to progressive system of drug delivery. In nanomedicine drug delivery system, nanoscale structures act as a carrier of various substances like nanorobots [166], sensory [167], delivery of drugs [168], natural polysaccharides [169, 170], antibodies [171], tunable surfactants [172], cell membrane [173], and peptides [174] to target regions and improve specificity of organisms through chemical functionalization. The system for controlled drug release through employment of different nano drug carriers is shown in Fig. 10.13. There are two main paths to deliver drugs through nanostructures: first is passive and second is self-delivery. In the foregoing, hydrophobic effect is being used to incorporate the drugs in structural cavity. When nanomaterials are employed toward specific sites, the proposed drug amount is allowed due to small content of drugs which is surrounded by hydrophobic contexture [175]. Moreover, the purposive drug is directly associated with nanocarrier for simple delivery. In this way, the drug releasing time is critical as the drug will dissociate from the MNPs before

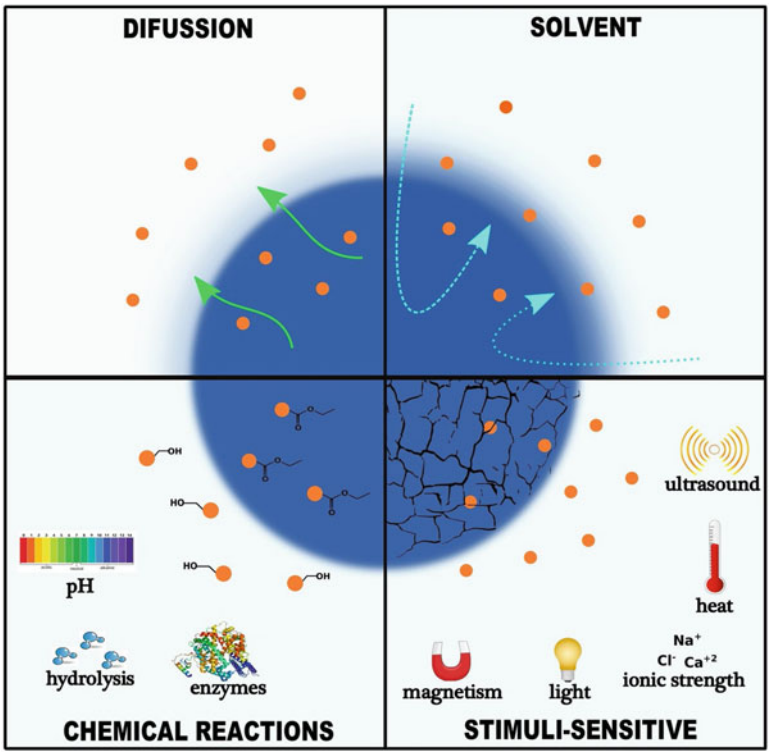

Fig. 10.13 Systems for drug release by employment of various nanocarriers. (Reprinted with permission from reference [177])

reaching to the desired target; however, its efficiency and bioactivity will be minimized if it is dissociated at right time from the nanocarrier [175]. Targeting of drugs is further classified into two aspects, active and passive, by usage of nanoformulations. In the mechanism of active targeting, moieties, such as peptides and antibodies, are associated with delivery system to hold them toward receptors of the target site. The passive targeting mechanism is a little bit different from active targeting because the desired drug carrier circulated in the bloodstream and propelled to the target site through affinity affected by properties like temperature, shape, pH, and molecular site. The receptors are primary targets on cell membranes, antigens on the surfaces of cell, and lipid elements of cell membrane [176]. Currently, drug deliveries based on nanoformulations are mostly directed toward the cure and treatments of cancer.

Hence, stimuli-responsive carriers at nanoscale exhibit capability to regulate the drug release through external actions such as pH [178], heat [179–181], ultrasound [182], light [183], magnetism [184, 185], and ionic strength [186], which help to enhance the targeting ability and control of dosage. For example, by using external magnetic field, superparamagnetic iron oxide nanoparticles are conjugated with lipids [187] or polymeric nanocarrier [188] to activate a controlled drug release

system. Furthermore, Ulbrich et al. proposed a recent attainment of drug delivery mechanisms, especially on basis of magnetic nanoparticles and polymeric nanoparticles and mark directions as well to the covalently and noncovalently conjugated drugs effects toward cure of cancer [189]. Besides it, Au/Fe_3O_4@polymer MNPs have been utilized for chemo-photothermal therapy application under the excitation of NIR light [190].

10.5.2 MNPs in Drug Delivery

Meaningful clinical investigations have been studied for the usage of MNPs especially iron oxide-based nanoparticles due to its unique properties for theranostics such as magnetic drug targeting, molecular imaging, and magnetic hyperthermia applications [117, 191–193]. In this section, we illustrate some important examples of magnetic iron oxide and iron-based nanoparticles in drug delivery system. Due to high response toward magnetic field of magnetic nanoparticles, it establishes them to penetrate in target site either by means of internally employment of permanent magnet or by applying external magnetic field [194]. Early in the 1970s, Widder et al. used the magnetic microspheres for the delivery of drugs toward tumor [195].

Cancer-related mortality is a very serious problem in this modern world because the uncontrolled abnormal cell accumulates and disseminates to normal healthy tissues [126]. Gao et al. proposed a synthesis of 8 nm of Fe_3O_4 nanoparticles and cisplatin which are dual loaded with magnetic liposome for generous ROS (Fig. 10.14) [196]. The apoptosis of mitochondria and DNA damage is caused by intracellular ROS, restoring the system in cisplatin-resistant A549 (A549/R) cells. In this work, novel magnetic liposome was designed, consisting of drug, targeting ligands, and iron oxide MNPs. The generation of Fe^{2+}/Fe^{3+} from Fe_3O_4 MNPs in the acid liposome causes to cisplatin and catalyzed anticancer drug artemisinin (ART) to form toxic ROS via Fenton reaction, which improved the cisplatin anticancer effect with much less side effects.

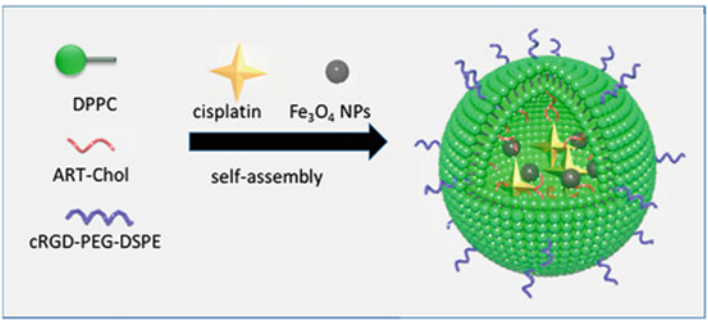

Fig. 10.14 Graphical synthesis mechanism of the magnetic liposomes cRGD-AFePt@NPs. (Reprinted with permission from reference [196])

Further the loading of cargos carrying Fe_3O_4 and cisplatin was estimated by respective formula.

$$\text{DLC (wt\%)} = \frac{\text{weight of cargos (cisplatin or Fe O NPs)}}{\text{weight of cRGD AFePt@NPs}}$$

In vitro examination of A549/R cells exhibits that cRGD-AFe@NPs showed a 15.17-fold lower IC_{50} value of cisplatin ($IC_{50} = 32.47$ μM). Furthermore, increased intracellular ROS formation and apoptosis of cell are showed by flow cytometry tests.

Various diseases can be cured with targeted drug delivery in better way by means of magnetic nanoparticles. According to the World Health Organization, cardiovascular diseases caused the death of 17.7 million people in 2015, a toll that comprises ~31% of mortality throughout the world [197]. Thrombolysis is the type of blood clot which may lead to different mortalities and disabilities as outcomes. Prilepskii et al. proposed a novel magnetic nanocomposite with thrombolytic drug synthesized by heparin-mediated cross-linking of urokinase (MNPs@uPA) [198].

This novel magnetic thrombolytic drug nanocomposite was synthesized by extension of urokinase-type plasminogen trigger to MNPs with heparin as the binding agent (Fig. 10.15a). This nanocomposite MNPs@uPA exhibits superparamagnetic behavior as shown in Fig. 10.15b. Subsequently, examine the nanocomposite on thrombolytic activity in clot model, found that in the presence of

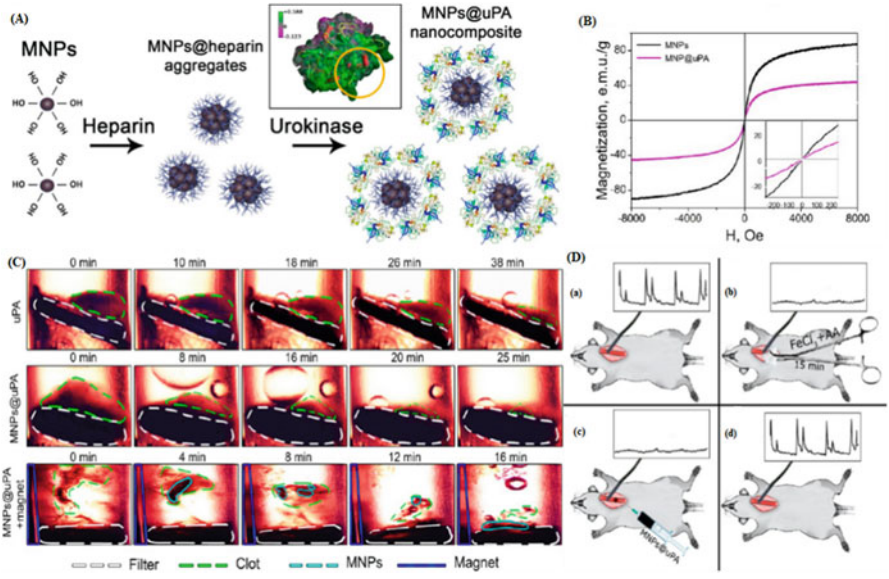

Fig. 10.15 (**a**) Synthesis process of MNPs@uPA. (**b**) Magnetic property (M-H) curve of MNPs@uPA and of pure magnetite. (**c**) Dissolution of the model clot exposed to nanoparticles. (**d**) Thrombolytic activity of MNPs@uPA in vivo. (Reprinted with permission from reference [198])

magnetic field the rate of clot reductions being carried out in 12 min with (MNPs@uPA) and take mean value of 5 measurements (Fig. 10.15c). Furthermore, the scheme (Fig. 10.15d) investigation of this novel thrombolytic drug composite is also examined in vitro. Firstly, in rat carotid artery clot was formed through imposing of cotton piece with ascorbic acid and $FeCl_3$. After injection of MNPs@uPA within 0.5–10 min, the blood flow resumed, and the gradual decline of clot continued. This new composition is FDA approved, and biocompatible components also exhibit thrombolytic efficiency by at least 30%.

As an improvement of hydrophobic drugs in vivo achievable by nanoparticle formulation through circumventing solubility effect and handover targeted delivery, Hsiao et al. presented a mechanism for hydrophobic drug PTX attached on the surface of hydrophobic iron oxide NPs and then coated with chitosan-PEG copolymer. Later, chlorotoxin (CTX) was attached onto the MNPs as a targeting agent. This work has significance to overcome the hurdles of hydrophobic drugs to the specific area, and IONPs easily manipulate with the external magnetic field which is another advantage of this work. The hydrophobic CTX drug contains 36-amino acid peptide and particularly enchains to metalloproteinase-2 (MMP-2) and was used for proposed human glioblastoma (GBM) cell. The synthesis mechanism is given in Fig. 10.16a. The prepared PTX-NPs are very stable and did not show any

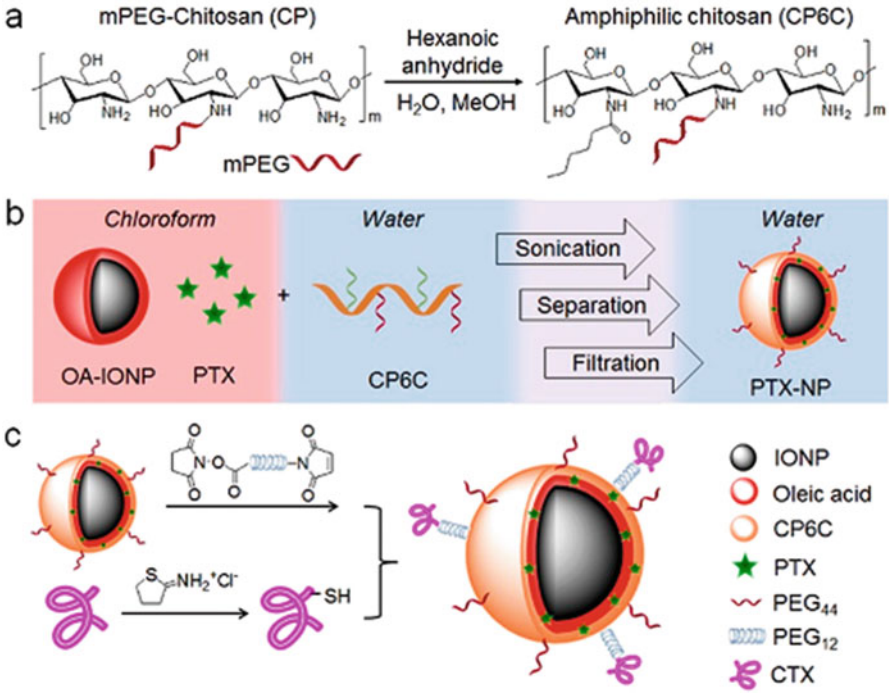

Fig. 10.16 Schematic description of preparation of CP6C copolymer-coated, PTX-loaded, and CTX-conjugated IONPs. (Reprinted with permission from reference [199])

aggregation in the hydrodynamic size measurements. On the other hand, most of the liposomes are to be left in serum at 37 °C for few hours [200–202]. Further, investigate the cellular uptake of NPs with the help of confocal laser scanning microscope (CLSM). While, nonspecific uptake of PTX-NP by cell was investigated which shows that biniding of CTX-PTX-NP accepted by cells which shows that binding of CTX refined the cellular uptake. Next, cell viability and the therapeutic performance were investigated on U-118 MG cells using different groups of synthesized MNPs. Accordingly, improved cellular drug growth-mediated mechanism by CTX in CTX-PTX-NP enhanced the killing of tumor cell. Further, CP6C copolymer-coated iron oxide nanoparticles are promising platform for hydrophobic drug delivery system and can be replaced with different ligands for imaging and targeting applications.

As with the passage of time, nanoparticles have gained much more attention toward delivery of vaccine to tumor cells. Furthermore, vaccine delivery system based on nanoformulation has great ability to enhance the vaccine immunogenicity.

Conventionally, the nanoparticle-adjuvant vaccine articulation is classified into two types. In the first type, nanoparticles acted as delivery system by delivery of antigen to immune system either by delivery of antigen to target site or through congesting by immune cell [204]. The remaining type is based on nanoparticles used as immune potentiator to improve antigen operation. Zhao et al. reported the mechanism of vaccine delivery based on coupling of Ovalbumin Endofit with iron oxide nanoparticles (Fe_3O_4-OVA) to inhibit the tumor growth [203]. In vitro cellular uptake of Fe_3O_4-OVA is being studied on treatment of CT26 cells for 24 h. Accordingly, tumor growth was remarkably inhibited through incubation of Fe_3O_4-OVA NPs against single Fe_3O_4 and soluble OVA which had comparable PBS control group (Fig. 10.17e). Additionally, the in vivo cytotoxicity of Fe_3O_4-OVA nanovaccine was studied, and intratumoral injection results showed that this nanovaccine has better compatibility after investigating organ toxicity (Fig. 10.17c). Results revealed that Fe_3O_4-OVA NPs have strong effect in immunity reaction and tumor ablation as well as can be employed as a general system for cancer vaccines.

10.6 Magnetic Resonance Imaging (MRI)

Worldwide scientists have been paying attention to improve the cancer diagnosis techniques at early stage by combining different scientific disciplines. Many molecular imaging techniques have been available for early diagnosis of serious injuries and different types of cancers. However, magnetic resonance imaging gained significant interest in clinical usage and for medical research purpose owing to its special features such as noninvasive, selectivity, and sensitivity as compared to other imaging modalities. This molecular imaging technique successfully maps severe injuries, abnormalities, heart problems, and cancer tumor [205, 206].

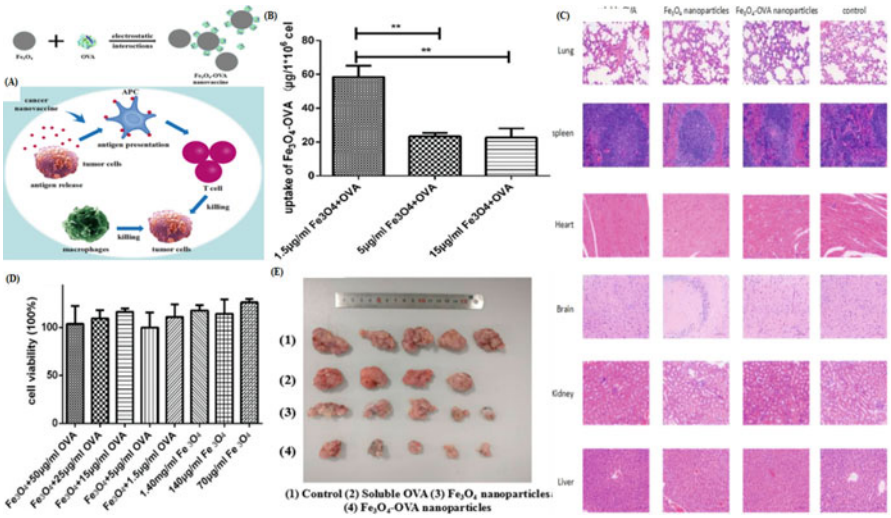

Fig. 10.17 (**a**) Schematic and working principle of Fe_3O_4-OVA. (**b**) The concentration of MNPs inside DCs cells. (**c**) Histological examination of different major organs treated with different groups of NPs. (**d**) Cell toxicity experiment. (**e**) Photograph of tumors after treatment. (Reprinted with permission from reference [203])

10.6.1 MRI Contract Agents

Initially, MRI was designed for imaging purpose because it does not contain any harmful radiations. However, low sensitivity was the major drawback of MRI when compared with another diagnosis technique such as nuclear imaging. Later, this shortcoming is resolved by the development of magnetic contrast agents (MCAs), and then MRI attained a significant position in clinical diagnosis which is a promising tool for biomedical research [207]. MCAs increase sensitivity and/or specificity because of the shortened relaxation time of protons. The relaxivity values of r_1 and r_2, which are generally measured in $mM^{-1}\ s^{-1}$, demonstrate the increase in $1/T_1$ and $1/T_2$ per concentration [M] of contrast agent, respectively. The expression is given below.

$$\frac{1}{T_i} = \frac{1}{T_{i,0}} + r_i[M]\ (i = 1, 2) \tag{10.8}$$

The efficiency of CAs in MRI is measured in expression of the ratio between the transverse and longitudinal relaxivities (r_2/r_1). CAs are strongly depending on this r_2/r_1 ratio because by using this, we can decide whether the CAs can be employed as a positive (T_1) or negative (T_2) agent.

Furthermore, from the clinical applications point of view, clinical contrast agents can be categorized into two types: (1) positive ones (blood pool agents, hepatobiliary agents, and extracellular agents) and (2) negative ones (blood pool imaging and passive targeting) [208]. Magnetic resonance probes are further categorized into two types: the first one is

paramagnetic material-based CAs such as gadolinium (Gd^{3+}) or manganese (Mn^{2+}) which are usually used as T_1 MR imaging, and the second type is based on superparamagnetic CAs such as pure iron oxide NPs and iron oxide-based NPs which are generally used for T_2 MR imaging. Paramagnetic agents are coupled with some chelate to control the toxicity of free ions. Sometimes polymer or coating substances are used to improve the biocompatibility and aggregation problems of the iron oxide NPs. Superparamagnetic agents have a considerably better magnetic moment as compared to paramagnetic agents [209, 210]. Mostly, these superparamagnetic iron oxide agents are used for T_2. However, a new class, ultrasmall (5 nm) iron oxide NP, has been introduced to increase the T_1 MR imaging [211, 212].

10.6.2 The Longitudinal Relaxation (T_1) Agents

Positive contrast agents decrease the T_1 and r_2/r_1 and generate bright image. Generally, gadolinium (III)-based complexes, which have seven unpaired electrons on the surface, are used to create T_1-weighted MRI. These ions enhance the relaxation rate of the adjacent and exchangeable water molecules and as a result increase the intensity in T_1-weighted images. The longitudinal relaxation reveals a thermal loss from the spin system to its surroundings (lattice). The intricated paramagnetic ion is embedded by three kinds of water molecule. Firstly, water molecules are attached directly to the paramagnetic ion at inner sphere. These kinds of molecules can exchange with the surrounding bulk water and generate the strongest effect on the overall relaxivity because of direct link with the paramagnetic ion. Hydrogen bonded to the organic chelate linking the paramagnetic ion at second sphere or middle sphere of the water molecule.

They experience fast exchange with the nearby bulk water, and their relaxivity is less affected. Finally, the outer sphere or bulk water including the water from surrounding the complex as the contrast agent diffuses through the tissue (Fig. 10.18).

The magnetization of paramagnetic materials is directly based on the number of ions and electrons of unpaired ions. The configuration of paramagnetic metal ions with magnetic moment is given in Table 10.1.

Some other transition metals also have unpaired ions, but they do not fulfill the requirement of Larmor frequency rule. However, ions of iron, manganese, and gadolinium perfectly meet the above requirements. The major difficulty is to decrease the toxicity effect of paramagnetic heavy metal ions. Several gadolinium (III)-based contrast agents have been available commercially, and the most common are (1) Magnevist (Bayer HealthCare Pharmaceuticals), (2) ProHance (Bracco Diagnostics), and (3) Omniscan (GE Healthcare). These complexes are all administered intravenously (0.1 mmol/Kg dose) and are pass out from the kidneys within 24 h. They enhanced image efficiency in the brain, lesions, abnormalities, associated tissues, and spine, but in pathogenic tissues, such as certain tumors, current contrast agents are not perfect in visualization.

Magnetic nanoparticles based on gadolinium and manganese have a quite stronger paramagnetic property in comparison with iron oxide nanoparticles. For

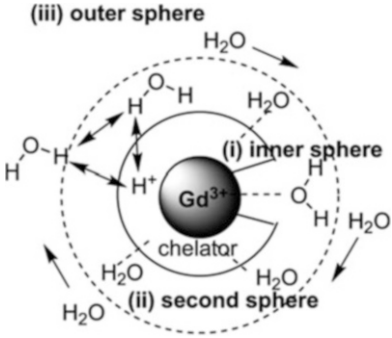

Fig. 10.18 The three types of water molecule which undergo a change in relaxivity when in proximity to a paramagnetic ion. (Reprinted with permission from reference [213])

Table 10.1 List of some important paramagnetic metal ions with their configuration and moment. (Reprinted with permission from reference [214])

Ion	Configuration	Magnetic moment
$^{24}Cr^{3+}$		3.9
$^{25}Mn^{2+}$		5.9
$^{26}Fe^{3+}$		5.9
$^{29}Cu^{2+}$		1.7
$^{63}Eu^{3+}$		3.4
$^{64}Gd^{3+}$		7.9
$^{66}Dy^{3+}$		10.6

example, in case of PEG (polyethylene glycol)-coated Gd_2O_3, the r_2/r_1 is around 1, while in commercial iron oxide nanoparticles (Feridex) as negative contrast agents, the r_2/r_1 value is about 10. Further, some Gd_2O_3 nanoparticles are more sensitive than clinical imaging CAs such as Gd-DOTA complex [215].

Apart from the Gd^{3+}-based contrast agents for T_1 MR imaging, recently Mn^{2+}-based nanoparticles have obtained a considerable attraction. Manganese is one kind of paramagnetic contrast agent which showed better efficiency in cardiac and hepatic MRI. Particularly, it is used to observe the mapping of functional brain regions and anatomical structures. In manganese case, cellular toxicity issues are still hurdle to be a perfect contrast agent [216]. Also, the unpaired electron of Mn^{2+} decreases its stability, and therefore it is very exciting to prepare the stable and homogeneous CAs based on manganese. The effective performance of manganese as a MCA is strongly based on the affected site-specific delivery and low dose to avoid the negative signal, maintaining the detectability by MRI.

Another paramagnetic contrast agent is Dy. Dye-based CAs are also extensively utilized as T_1 contrast agents due to high value of intrinsic paramagnetism of lanthanide ion. Hydrophilic Dy^{3+} agent coated by amphiphilic polymers linked with liposome enhances the visualization ability in cellular epitopes even at very low concentrations. Moreover, at 7 T, unilamellar liposome loaded with Dy-HPDO3A shows T_2 relaxation enhancement as compared to superparamagnetic iron oxide nanoparticles [65, 217].

Importantly, in the recent years, the Food and Drug Administration (FDA) authority has added a warning notice on gadolinium CA injection because of increasing the risk of nephrogenic fibrosing dermopathy (NFD) and nephrogenic systemic fibrosis (NSF) for patients who have renal failure problem. These patients are encouraged to find the alternative CAs instead of Gd^{3+}. This kind of disease can cause fibrosis of the joints, internal organs, eyes, and skin which if stern enough may lead to the patient's death. The abovementioned diseases are associated with Omniscan contrast agent, a nonionic linear agent, which has $Kd = 1.4 \times 10^{-17}$ M and shows poor kinetic stability for Gd^{3+} and is easily released into the blood. The contrast agents with poor kinetic stability are easy to discharge in the kidneys due to lower pH value as compared to surrounding tissues. Recently, new research work has carried out Gd(III)-DTPA chelates with dendrimer [218, 219].

10.6.3 The Transverse Relaxation (T2) Agents

Iron oxide nanoparticles present the superparamagnetic behavior which is significant for T_2 dark (negative) contrast on MRI in comparison with paramagnetic ions. The aptitude of SPIONs to achieve as MR imaging CAs is aggressively examined in the last 20 years. MNPs with controlled shape, size, and magnetic features are intensively studied as MRI contrast agents. However, several other organic or inorganic layers have been established to increase their stability, functionalization, targeting, and toxicity. Most SPION-based clinical-approved MRI contrast agents are coated with dextran citrate-stabilized particles (VSOP-C184) or carbohydrate [220, 221]. Some polymers, metals, and silica are also in development phase or in different stages of the preclinical research. The versatile coating layers provided nanoparticles as platform for additional fictionalization by conjugation with multi-domain targeting entities such as peptides and antibodies. The magnetic moment of SPIONPs is much higher than paramagnetic and consequently needs a low concentration for the contrast agent purposes. In the last two decades, several reports have demonstrated the detailed investigation on the iron oxide, iron oxide cores with different sizes, and their applications in theranostics [222]. The controls over size, shape, and magnetic, intrinsic, and extrinsic properties of the nanoparticles are major factors to develop excellent T_2 contrast agents. It is obvious, MNPs showed contrast enhancment under applied alternative magnetic fields compare with water [223].

It is observed that there was no dipole moment in the absence of magnetic field, and by applying an external field, the MNPs induced magnetic dipole moment in the surrounding water molecules. And it results in the shortening of the spin-spin relaxation time of the proton. Various concentrations of MNPs are uptaken by different tissues with variable T_2 values and create distinct MR images. Healthy cells contain an effective reticuloendothelial system (RES) as compared to the cancerous cells. Therefore the relaxation time of the tumor cells will not have reformed by the CAs. These phenomena make them apparent from the adjacent healthy cells [224].

MNPs of iron oxide are confirmed to be a better substitution for the gadolinium-based complexes like Gd-DTPA as CAs owing to their high relaxivity, biocompatibility, and low toxicity [225]. Therefore, little dose of SPIONPs was required into the human body than paramagnetic material-based CAs. Currently, commercialized available gadolinium required 10-7 mol/g to obtain high-quality image which is very high, and typical receptors usually need low concentrations of 10^{-9} to 10^{-13} mol/g. Therefore, it is very important to resolve the sensitivity issue. Many MNPs have been under investigation as CAs, but magnetite is a well-examined material with very low toxicity and rapidly cleared from the organism [226]. Wittenberg performed a very refined and detailed research on different sizes, their effects on magnetization, and relaxivities of MRI as shown in Fig. 10.19. When the particle size is increasing, the T_2-weighted contrast is enhanced significantly. In order to increase the biocompatibility, inorganic oxides (silica and carbon), organic surfactants (dodecylamine and sodium oleate), organic polymers (chitosan, dextran, polyethylene glycol, polyaniline, and polysorbate), inorganic metals (gold), as well as bioactive structures and molecules (ligands/receptors, liposomes, and peptides) have been introduced on the surface of magnetic nanoparticles [227].

The aggregation and embolization are the important issues related to MNPs that start to restrict blood flow. In addition, most of the MNPs entered in the liver and produced cytotoxicity which is another unwanted side effect. Small particles with biodegradable coating substance provide a platform to overcome these circumstances. Previous studies have shown that 15.0 nm nanoparticles tend to be cleared by the liver, whereas ultrasmall particles (5.0 nm) can be excreted quickly by the kidney [228].

10.7 Conclusion and Prospective

Nanotechnology holds an immense potential in energy, agriculture, and environmental and biomedical applications. Nanomaterials offer a significant opportunity to ease the daily life from traditional to modern. Engineered magnetic nanoparticles present multiple solutions for the diagnosis and treatment of many dangerous diseases due to their unique characteristics. The magnetic characteristics of single-domain iron oxide nanoparticles are strongly based on the saturation magnetization, nanoparticle size and aggregation, Néel relaxation time, and anisotropy constant.

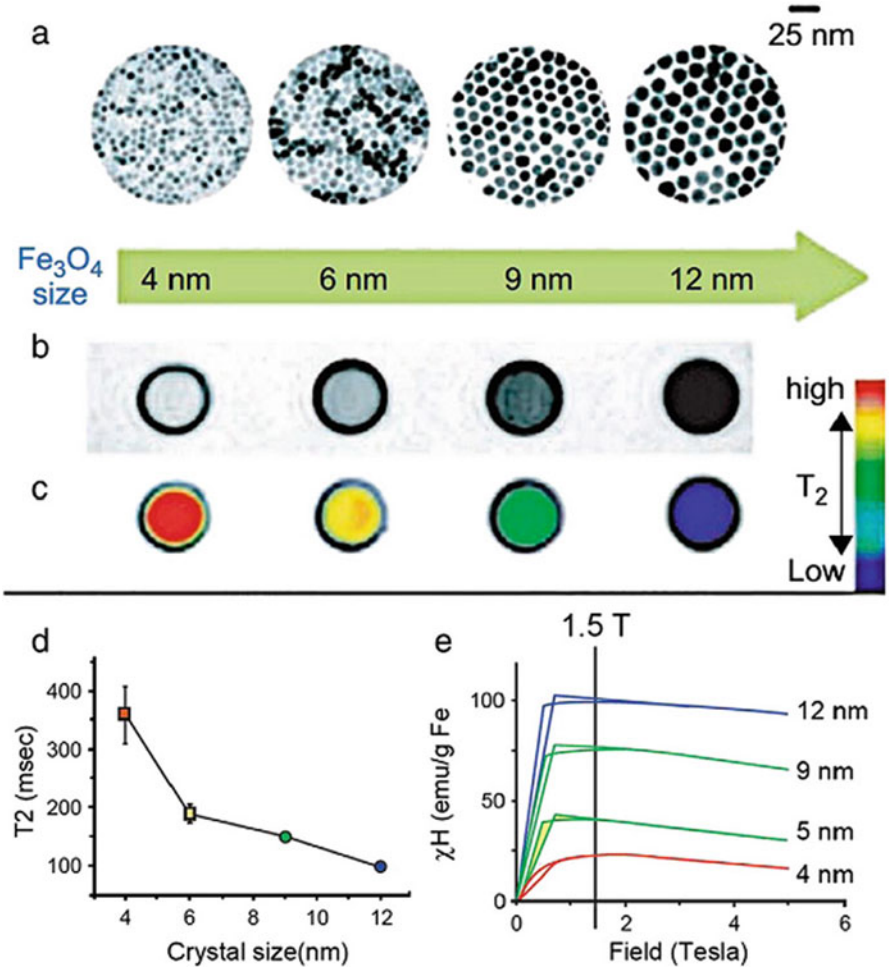

Fig. 10.19 (**a**) TEM images of nanoparticles of Fe_3O_4 nanoparticle of different sizes, (**b**, **c**) size-based T_2 characteristics and (**d**) T_2 values with respect to size, and (**e**) magnetization characteristics according to size [229]

MNPs have showed hyperthermia effect by applying an alternative field, that is, activation of MNP brings targeted therapeutic heating of tumor. MNPs actively participated as a therapeutic agent, but there is still a need to consider the size-dependent temperature change. Also, mostly studies explained about the intratumor killing effect, therefore, intravenous targeting and produce hyperthermia inside cancer cell will be remarkable edition in the field on cancer theranostics. Delivery systems using magnetic nanoparticles are promising drug transporter. However, there is still a need to develop some accurate methods to improve the delivery efficiency that is needed to have proper surface functionalities, achieving a

maximum targeted delivery of drugs. These properties of the magnetic nanoparticles play a significant character where these features are essential not only in MR imaging and relaxivities properties of T_1- and T_2-weighted contrast agents but also are potential applicability in medical areas. Finally, the improvement of synthesizing magnetic nanoparticle probes is still in its infancy, but it has contributed a lot in developing MRI. The use of nanoparticles as contrast agents, advancing toward clinical implementation, to improve the relaxivity coefficient, long-term cytotoxicology, storage, and kinetic stability, should continue to be taken into consideration.

Acknowledgments The authors would like to thank the continuous support by National Key R&D Program of China (2018YFC0910601), Natural Science Foundation of China (U1432114 to Aiguo Wu and 81950410638 and 81650410654 to M. Zubair Iqbal), Zhejiang Province Financial Supporting (2017C03042, LY18H180011), and the Science & Technology Bureau of Ningbo City (2015B11002, 2017C110022). Furthermore, the authors also acknowledge Shanghai Synchrotron Radiation Facility at Line BL15U (No. h15 sr0021) used for X-ray fluorescence imaging and National Synchrotron Radiation Laboratory in Hefei used for soft X-ray imaging (No. 2016-HLS-PT-002193).

References

1. Baker JR, Quintana A, Piehler L, Banazak-Holl M, Tomalia D, Raczka E. The synthesis and testing of anti-Cancer therapeutic Nanodevices. Biomed Microdevices. 2001;3:61–9.
2. Savage N, Thomas TA, Duncan JS. Nanotechnology applications and implications research supported by the US Environmental Protection Agency STAR grants program. J Environ Monit. 2007;9:1046–54.
3. Martin CR. Welcome to nanomedicine. Nanomedicine. 2006;1:5.
4. Sonawane GH, Patil SP, Sonawane SH. Chapter 1 - Nanocomposites and its applications. In: Mohan Bhagyaraj S, Oluwafemi OS, Kalarikkal N, Thomas S, editors. Applications of nanomaterials. Cambridge, UK: Woodhead Publishing; 2018. p. 1–22.
5. Rahman M, Rebrov E. Microreactors for gold nanoparticles synthesis: from faraday to flow. PRO. 2014;2:466.
6. Schoonman J. Nanostructured materials in solid state ionics. Solid State Ion. 2000;135:5–19.
7. Rabia Riasat NG, Riasat Z, Aslam I, Sakeena M. Effects of nanoparticles on gastrointestinal disorders and therapy. J Clin Toxicol. 2014;6:10.
8. Iqbal MZ, Wang F, Zhao H, Rafique MY, Wang J, Li Q. Structural and electrochemical properties of SnO nanoflowers as an anode material for lithium ion batteries. Scr Mater. 2012;67:665–8.
9. Iqbal MZ, Wang F, Feng T, Zhao H, Rafique MY, Rafi ud D, Farooq MH, Javed Q u a J, Khan DF. Facile synthesis of self-assembled SnO nano-square sheets and hydrogen absorption characteristics. Mater Res Bull. 2012;47:3902–7.
10. Salata OV. Applications of nanoparticles in biology and medicine. J Nanobiotechnol. 2004;2:3–3.
11. Yang L, Zhang X, Ye M, Jiang J, Yang R, Fu T, Chen Y, Wang K, Liu C, Tan W. Aptamer-conjugated nanomaterials and their applications. Adv Drug Deliv Rev. 2011;63:1361–70.
12. Reeves DB, Weaver JB. Approaches for modeling magnetic nanoparticle dynamics. Crit Rev Biomed Eng. 2014;42:85–93.
13. Gun'ko Y. Magnetic nanomaterials and their applications. Nano. 2014;4:505.

14. Al Lehyani SHA, Hassan R, Alharbi AA, Alomayri T, Alamri H. Magnetic hyperthermia using cobalt ferrite nanoparticles: the influence of particle size. Research Article. Int J Adv Tech. 2017;8:6.
15. Pankhurst QA, Connolly J, Jones SK, Dobson J. Applications of magnetic nanoparticles in biomedicine. J Phys D Appl Phys. 2003;36:R167.
16. Malekigorji M, Curtis ADM, Hoskins C. The use of iron oxide nanoparticles for pancreatic cancer therapy. J Nanomed Res. 2014;1:12.
17. Lee H, Shin T-H, Cheon J, Weissleder R. Recent developments in magnetic diagnostic systems. Chem Rev. 2015;115:10690–724.
18. Ito A, Shinkai M, Honda H, Kobayashi T. Medical application of functionalized magnetic nanoparticles. J Biosci Bioeng. 2005;100:1–11.
19. Masih D, Frank S, Joachim L, Nathalie R, Biplab S, Werner K, Heiko W. Nanoscale size effect on surface spin canting in iron oxide nanoparticles synthesized by the microemulsion method. J Phys D Appl Phys. 2012;45:195001.
20. Kai W, Liang T, Diqing S, Jian-Ping W. Magnetic dynamics of ferrofluids: mathematical models and experimental investigations. J Phys D Appl Phys. 2017;50:085005.
21. Kim T, Shima M. Reduced magnetization in magnetic oxide nanoparticles. J Appl Phys. 2007;101:09M516.
22. Dutta P, Pal S, Seehra MS, Shah N, Huffman GP. Size dependence of magnetic parameters and surface disorder in magnetite nanoparticles. J Appl Phys. 2009;105:07B501.
23. Demortière A, Panissod P, Pichon BP, Pourroy G, Guillon D, Donnio B, Bégin-Colin S. Size-dependent properties of magnetic iron oxide nanocrystals. Nanoscale. 2011;3:225–32.
24. Teja AS, Koh P-Y. Synthesis, properties, and applications of magnetic iron oxide nanoparticles. Prog Cryst Growth Charact Mater. 2009;55:22–45.
25. Lu A-H, Salabas EL, Schüth F. Magnetic nanoparticles: synthesis, protection, functionalization, and application. Angew Chem Int Ed. 2007;46:1222–44.
26. Mohammadzadeh A, Sadri M, Seyed Afghahi SS, Alizadeh Y, Najafian S, Hosseini H. In vitro biocompatibility of low and medium molecular weight chitosan–coated Fe3O4 nanoparticles. Nanomed Res J. 2017;2:250–9.
27. Atila Dinçer C, Yildiz N, Karakeçili A, Aydoğan N, Çalimli A. Synthesis and characterization of Fe3O4-MPTMS-PLGA nanocomposites for anticancer drug loading and release studies. Artif Cells Nanomed Biotechnol. 2017;45:1408–14.
28. Jeun M, Lee S, Kang JK, Tomitaka A, Kang KW, Kim YI, Takemura Y, Chung K-W, Kwak J, Bae S. Physical limits of pure superparamagnetic Fe3O4 nanoparticles for a local hyperthermia agent in nanomedicine. Appl Phys Lett. 2012;100:092406.
29. Ma P, Luo Q, Chen J, Gan Y, Du J, Ding S, Xi Z, Yang X. Intraperitoneal injection of magnetic Fe_3O_4-nanoparticle induces hepatic and renal tissue injury via oxidative stress in mice. Int J Nanomedicine. 2012;7:4809–18.
30. Patil JV, Mali SS, Kamble AS, Hong CK, Kim JH, Patil PS. Electrospinning: a versatile technique for making of 1D growth of nanostructured nanofibers and its applications: An experimental approach. Appl Surf Sci. 2017;423:641–74.
31. Khan I, Saeed K, Khan I. Nanoparticles: properties, applications and toxicities. Arab J Chem. 2017; https://doi.org/10.1016/j.arabjc.2017.05.011.
32. Goel S, Chen F, Cai W. Synthesis and biomedical applications of copper sulfide nanoparticles: from sensors to theranostics. Small (Weinheim an der Bergstrasse, Germany). 2014;10:631–45.
33. Annu, Ali A, Ahmed S. Green synthesis of metal, metal oxide nanoparticles, and their various applications. In: Martínez LMT, Kharissova OV, Kharisov BI, editors. Handbook of ecomaterials. Cham: Springer; 2018. p. 1–45.
34. Grill L, Dyer M, Lafferentz L, Persson M, Peters MV, Hecht S. Nano-architectures by covalent assembly of molecular building blocks. Nat Nanotechnol. 2007;2:687.
35. Ikkala O, ten Brinke G. Functional materials based on self-assembly of polymeric Supramolecules. Science. 2002;295:2407–9.

36. Rawat RS. Dense plasma focus-from alternative fusion source to versatile high energy density plasma source for plasma nanotechnology. J Phys Conf Ser. 2015;591:25.
37. Sun S, Murray CB, Weller D, Folks L, Moser A. Monodisperse FePt nanoparticles and ferromagnetic FePt nanocrystal superlattices. Science. 2000;287:1989–92.
38. Shevchenko EV, Talapin DV, Rogach AL, Kornowski A, Haase M, Weller H. Colloidal synthesis and self-assembly of CoPt3 nanocrystals [J. Am. Chem. Soc. 2002, 124, 11480−11485]. J Am Chem Soc. 2002(124):13958.
39. Park J, An K, Hwang Y, Park J-G, Noh H-J, Kim J-Y, Park J-H, Hwang N-M, Hyeon T. Ultra-large-scale syntheses of monodisperse nanocrystals. Nat Mater. 2004;3:891.
40. Armijo LM, Brandt YI, Mathew D, Yadav S, Maestas S, Rivera AC, Cook NC, Withers NJ, Smolyakov GA, Adolphi NL, Monson TC, Huber DL, Smyth HDC, Osiński M. Iron oxide nanocrystals for magnetic hyperthermia applications. Nano. 2012;2:134.
41. Grasset F, Labhsetwar N, Li D, Park DC, Saito N, Haneda H, Cador O, Roisnel T, Mornet S, Duguet E, Portier J, Etourneau J. Synthesis and magnetic characterization of zinc ferrite nanoparticles with different environments: powder, colloidal solution, and zinc ferrite−silica Core−Shell nanoparticles. Langmuir. 2002;18:8209–16.
42. Park S-J, Kim S, Lee S, Khim ZG, Char K, Hyeon T. Synthesis and magnetic studies of uniform Iron Nanorods and Nanospheres. J Am Chem Soc. 2000;122:8581–2.
43. Puntes VF, Krishnan KM, Alivisatos AP. Colloidal nanocrystal shape and size control: the case of cobalt. Science. 2001;291:2115–7.
44. Benjamin JS. Dispersion strengthened superalloys by mechanical alloying. Metall Trans. 1970;1:2943–51.
45. Lukashev RV, Alekova AF, Korchagina SK, Chibirova FK. Mechanical processing of γ-Fe2O3. Inorg Mater. 2015;51:134–7.
46. Arbain R, Othman M, Palaniandy S. Preparation of iron oxide nanoparticles by mechanical milling. Miner Eng. 2011;24:1–9.
47. Chen C-N, Chen Y-L, Tseng WJ. Surfactant-assisted de-agglomeration of graphite nanoparticles by wet ball mixing. J Mater Process Technol. 2007;190:61–4.
48. Jiang Y, Liu J, Suri PK, Kennedy G, Thadhani NN, Flannigan DJ, Wang J-P. Preparation of an α''-Fe16N2 magnet via a ball milling and shock compaction approach. Adv Eng Mat. 2016;18:1009–16.
49. Chakka VM, Altuncevahir B, Jin ZQ, Li Y, Liu JP. Magnetic nanoparticles produced by surfactant-assisted ball milling. J Appl Phys. 2006;99:08E912.
50. Yiping W, Yang L, Chuanbing R, Liu JP. Sm–co hard magnetic nanoparticles prepared by surfactant-assisted ball milling. Nanotechnology. 2007;18:465701.
51. Kim EH, Lee HS, Kwak BK, Kim B-K. Synthesis of ferrofluid with magnetic nanoparticles by sonochemical method for MRI contrast agent. J Magn Magn Mater. 2005;289:328–30.
52. De Matteis L, Custardoy L, Fernández-Pacheco R, Magén C, de la Fuente JM, Marquina C, Ibarra MR. Ultrathin MgO coating of superparamagnetic magnetite nanoparticles by combined coprecipitation and sol–gel synthesis. Chem Mater. 2012;24:451–6.
53. Xie C-Y, Meng S-X, Xue L-H, Bai R-X, Yang X, Wang Y, Qiu Z-P, Binks BP, Guo T, Meng T. Light and magnetic dual-responsive Pickering emulsion micro-reactors. Langmuir. 2017;33:14139–48.
54. Salazar-Alvarez G, Muhammed M, Zagorodni AA. Novel flow injection synthesis of iron oxide nanoparticles with narrow size distribution. Chem Eng Sci. 2006;61:4625–33.
55. Basak S, Chen D-R, Biswas P. Electrospray of ionic precursor solutions to synthesize iron oxide nanoparticles: modified scaling law. Chem Eng Sci. 2007;62:1263–8.
56. Rasekh M, Ahmad Z, Cross R, Hernández-Gil J, Wilton-Ely JD, Miller PW. Facile preparation of drug-loaded tristearin encapsulated superparamagnetic iron oxide nanoparticles using coaxial electrospray processing. Mol Pharm. 2017;14:2010–23.
57. Zhang Y, Yang Y, Duan H, Lü C. Mussel-inspired catechol-formaldehyde resin coated Fe3O4 Core-Shell magnetic Nanospheres: An effective catalyst support for highly active palladium nanoparticles. ACS Appl Mater Interfaces. 2018;10:44535.

58. Unni M, Uhl AM, Savliwala S, Savitzky BH, Dhavalikar R, Garraud N, Arnold DP, Kourkoutis LF, Andrew JS, Rinaldi C. Thermal decomposition synthesis of iron oxide nanoparticles with diminished magnetic dead layer by controlled addition of oxygen. ACS Nano. 2017;11:2284–303.
59. De Palma R, Peeters S, Van Bael MJ, Van den Rul H, Bonroy K, Laureyn W, Mullens J, Borghs G, Maes G. Silane ligand exchange to make hydrophobic superparamagnetic nanoparticles water-dispersible. Chem Mater. 2007;19:1821–31.
60. Shevchenko EV, Talapin DV, Rogach AL, Kornowski A, Haase M, Weller H. Colloidal synthesis and self-assembly of CoPt3 nanocrystals. J Am Chem Soc. 2002;124:11480–5.
61. Chen D, Zhang Y, Chen B, Kang Z. Coupling effect of microwave and mechanical forces during the synthesis of ferrite nanoparticles by microwave-assisted ball milling. Ind Eng Chem Res. 2013;52:14179–84.
62. Iida H, Takayanagi K, Nakanishi T, Osaka T. Synthesis of Fe3O4 nanoparticles with various sizes and magnetic properties by controlled hydrolysis. J Colloid Interface Sci. 2007;314:274–80.
63. Shen Z, Chen T, Ma X, Ren W, Zhou Z, Zhu G, Zhang A, Liu Y, Song J, Li Z, Ruan H, Fan W, Lin L, Munasinghe J, Chen X, Wu A. Multifunctional Theranostic nanoparticles based on exceedingly small magnetic Iron oxide nanoparticles for T1-weighted magnetic resonance imaging and chemotherapy. ACS Nano. 2017;11:10992–1004.
64. Barrow M, Taylor A, García Carrión J, Mandal P, Park BK, Poptani H, Murray P, Rosseinsky MJ, Adams DJ. Co-precipitation of DEAE-dextran coated SPIONs: how synthesis conditions affect particle properties, stem cell labelling and MR contrast. Contrast Media Mol Imaging. 2016;11:362–70.
65. Sato T, Iijima T, Seki M, Inagaki N. Magnetic properties of ultrafine ferrite particles. J Magn Magn Mater. 1987;65:252–6.
66. Berkowitz A, Schuele W, Flanders P. Influence of crystallite size on the magnetic properties of acicular γ-Fe2O3 particles. J Appl Phys. 1968;39:1261–3.
67. Morales M, Andres-Verges M, Veintemillas-Verdaguer S, Montero M, Serna C. Structural effects on the magnetic properties of γ-Fe2O3 nanoparticles. J Magn Magn Mater. 1999;203:146–8.
68. Coey JMD. Noncollinear spin arrangement in ultrafine ferrimagnetic crystallites. Phys Rev Lett. 1971;27:1140.
69. Sun S, Zeng H. Size-controlled synthesis of magnetite nanoparticles. J Am Chem Soc. 2002;124:8204–5.
70. Xie J, Xu C, Kohler N, Hou Y, Sun S. Controlled PEGylation of monodisperse Fe3O4 nanoparticles for reduced non-specific uptake by macrophage cells. Adv Mater. 2007;19:3163–6.
71. Sun S, Zeng H, Robinson DB, Raoux S, Rice PM, Wang SX, Li G. Monodisperse mfe 2o4 (m= fe, co, mn) nanoparticles. J Am Chem Soc. 2004;126:273–9.
72. Peng X, Wickham J, Alivisatos A. Kinetics of II-VI and III-V colloidal semiconductor nanocrystal growth: "focusing" of size distributions. J Am Chem Soc. 1998;120:5343–4.
73. O'Brien S, Brus L, Murray CB. Synthesis of monodisperse nanoparticles of barium titanate: toward a generalized strategy of oxide nanoparticle synthesis. J Am Chem Soc. 2001;123:12085–6.
74. Redl FX, Black CT, Papaefthymiou GC, Sandstrom RL, Yin M, Zeng H, Murray CB, O'Brien SP. Magnetic, electronic, and structural characterization of nonstoichiometric iron oxides at the nanoscale. J Am Chem Soc. 2004;126:14583–99.
75. Rockenberger J, Scher EC, Alivisatos AP. A new nonhydrolytic single-precursor approach to surfactant-capped nanocrystals of transition metal oxides. J Am Chem Soc. 1999;121:11595–6.
76. Samia AC, Hyzer K, Schlueter JA, Qin C-J, Jiang JS, Bader SD, Lin X-M. Ligand effect on the growth and the digestion of co nanocrystals. J Am Chem Soc. 2005;127:4126–7.

77. Li Y, Afzaal M, O'Brien P. The synthesis of amine-capped magnetic (Fe, Mn, Co, Ni) oxide nanocrystals and their surface modification for aqueous dispersibility. J Mater Chem. 2006;16:2175–80.
78. Jana NR, Chen Y, Peng X. Size-and shape-controlled magnetic (Cr, Mn, Fe, Co, Ni) oxide nanocrystals via a simple and general approach. Chem Mater. 2004;16:3931–5.
79. Zeng H, Rice PM, Wang SX, Sun S. Shape-controlled synthesis and shape-induced texture of MnFe2O4 nanoparticles. J Am Chem Soc. 2004;126:11458–9.
80. Maity D, Ding J, Xue J-M. Synthesis of magnetite nanoparticles by thermal decomposition: time, temperature, surfactant and solvent effects. Funct Mater Lett. 2008;1:189–93.
81. Kahlweit M. Ostwald ripening of precipitates. Adv Colloid Interf Sci. 1975;5:1–35.
82. LaMer VK, Dinegar RH. Theory, production and mechanism of formation of monodispersed hydrosols. J Am Chem Soc. 1950;72:4847–54.
83. Groult H, Poupard N, Herranz F, Conforto E, Bridiau N, Sannier F, Bordenave S, Piot J-M, Ruiz-Cabello J, Fruitier-Arnaudin I. Family of bioactive heparin-coated iron oxide nanoparticles with positive contrast in magnetic resonance imaging for specific biomedical applications. Biomacromolecules. 2017;18:3156–67.
84. Mahmoudi M, Sahraian MA, Shokrgozar MA, Laurent S. Superparamagnetic iron oxide nanoparticles: promises for diagnosis and treatment of multiple sclerosis. ACS Chem Neurosci. 2011;2:118–40.
85. Huang K-W, Chieh J-J, Yeh C-K, Liao S-H, Lee Y-Y, Hsiao P-Y, Wei W-C, Yang H-C, Horng H-E. Ultrasound-induced magnetic imaging of tumors targeted by biofunctional magnetic nanoparticles. ACS Nano. 2017;11:3030–7.
86. Wang Y-XJ, Hussain SM, Krestin GP. Superparamagnetic iron oxide contrast agents: physicochemical characteristics and applications in MR imaging. Eur Radiol. 2001;11:2319–31.
87. Lu M, Cohen MH, Rieves D, Pazdur R. FDA report: ferumoxytol for intravenous iron therapy in adult patients with chronic kidney disease. Am J Hematol. 2010;85:315–9.
88. Hufschmid R, Arami H, Ferguson RM, Gonzales M, Teeman E, Brush LN, Browning ND, Krishnan KM. Synthesis of phase-pure and monodisperse iron oxide nanoparticles by thermal decomposition. Nanoscale. 2015;7:11142–54.
89. Iqbal MZ, Ma X, Chen T, Zhang L e, Ren W, Xiang L, Wu A. Silica-coated super-paramagnetic iron oxide nanoparticles (SPIONPs): a new type contrast agent of T 1 magnetic resonance imaging (MRI). J Mater Chem B. 2015;3:5172–81.
90. Song Q, Zhang ZJ. Shape control and associated magnetic properties of spinel cobalt ferrite nanocrystals. J Am Chem Soc. 2004;126:6164–8.
91. Wetz F, Soulantica K, Falqui A, Respaud M, Snoeck E, Chaudret B. Hybrid co–au nanorods: controlling au nucleation and location. Angew Chem Int Ed. 2007;46:7079–81.
92. Puntes VF, Zanchet D, Erdonmez CK, Alivisatos AP. Synthesis of hcp-co nanodisks. J Am Chem Soc. 2002;124:12874–80.
93. Mao B, Kang Z, Wang E, Lian S, Gao L, Tian C, Wang C. Synthesis of magnetite octahedrons from iron powders through a mild hydrothermal method. Mater Res Bull. 2006;41:2226–31.
94. Zhu H, Yang D, Zhu L. Hydrothermal growth and characterization of magnetite (Fe3O4) thin films. Surf Coat Technol. 2007;201:5870–4.
95. Giri S, Samanta S, Maji S, Ganguli S, Bhaumik A. Magnetic properties of α-Fe2O3 nanoparticle synthesized by a new hydrothermal method. J Magn Magn Mater. 2005;285:296–302.
96. Sobal NS, Hilgendorff M, Moehwald H, Giersig M, Spasova M, Radetic T, Farle M. Synthesis and structure of colloidal bimetallic nanocrystals: the non-alloying system ag/co. Nano Lett. 2002;2:621–4.
97. Chen D, Xu R. Hydrothermal synthesis and characterization of nanocrystalline Fe3O4 powders. Mater Res Bull. 1998;33:1015–21.
98. Xuan S, Wang F, Wang Y-XJ, Jimmy CY, Leung KC-F. Facile synthesis of size-controllable monodispersed ferrite nanospheres. J Mater Chem. 2010;20:5086–94.
99. Wu W, Wu Z, Yu T, Jiang C, Kim W-S. Recent progress on magnetic iron oxide nanoparticles: synthesis, surface functional strategies and biomedical applications. Sci Technol Adv Mater. 2015;16:023501.

100. Xuan S, Wang Y-XJ, Yu JC, Cham-Fai Leung K. Tuning the grain size and particle size of superparamagnetic Fe3O4 microparticles. Chem Mater. 2009;21:5079–87.
101. Kim J, Tran VT, Oh S, Kim C-S, Hong JC, Kim S, Joo Y-S, Mun S, Kim M-H, Jung J-W. Scalable Solvothermal synthesis of superparamagnetic Fe3O4 nanoclusters for bio-separation and Theragnostic probes. ACS Appl Mater Interfaces. 2018;10:41935.
102. Jalajerdi R, Gholamian F, Shafie H, Moraveji A, Ghanbari D. Thermal and magnetic characteristics of cellulose acetate-Fe3O4. J Nanostruct. 2011;1:105–9.
103. Ghanbari D, Salavati-Niasari M. Hydrothermal synthesis of different morphologies of MgFe 2 O 4 and magnetic cellulose acetate nanocomposite. Korean J Chem Eng. 2015;32:903–10.
104. Ghanbari D, Salavati-Niasari M, Sabet M. Preparation of flower-like magnesium hydroxide nanostructure and its influence on the thermal stability of poly vinyl acetate and poly vinyl alcohol. Compos Part B. 2013;45:550–5.
105. Hedayati K, Goodarzi M, Ghanbari D. Hydrothermal synthesis of Fe3O4 nanoparticles and flame resistance magnetic poly styrene nanocomposite. J Nanostruct. 2017;7:32–9.
106. Li J, Pei Q, Wang R, Zhou Y, Zhang Z, Cao Q, Wang D, Mi W, Du Y. Enhanced photocatalytic performance through magnetic field boosting carrier transport. ACS Nano. 2018;12:3351–9.
107. Kim J, Tran VT, Oh S, Kim C-S, Hong JC, Kim S, Joo Y-S, Mun S, Kim M-H, Jung J-W, Lee J, Kang YS, Koo J-W, Lee J. Scalable Solvothermal synthesis of superparamagnetic Fe3O4 nanoclusters for bioseparation and Theragnostic probes. ACS Appl Mater Interfaces. 2018;10:41935–46.
108. West JL, Halas NJ. Applications of nanotechnology to biotechnology: commentary. Curr Opin Biotechnol. 2000;11:215–7.
109. Davis S. Biomedical applications of nanotechnology—implications for drug targeting and gene therapy. Trends Biotechnol. 1997;15:217–24.
110. Hussein AK. Applications of nanotechnology in renewable energies—a comprehensive overview and understanding. Renew Sust Energ Rev. 2015;42:460–76.
111. Li X, Zhang F, Zhao D. Lab on upconversion nanoparticles: optical properties and applications engineering via designed nanostructure. Chem Soc Rev. 2015;44:1346–78.
112. Pfeiffer C, Rehbock C, Hühn D, Carrillo-Carrion C, de Aberasturi DJ, Merk V, Barcikowski S, Parak WJ. Interaction of colloidal nanoparticles with their local environment: the (ionic) nanoenvironment around nanoparticles is different from bulk and determines the physicochemical properties of the nanoparticles. J R Soc Interface. 2014;11:20130931.
113. Kelly KL, Coronado E, Zhao LL, Schatz GC. The optical properties of metal nanoparticles: the influence of size, shape, and dielectric environment. J Phys Chem B. 2003;107(3):668–77.
114. Gupta AK, Gupta M. Synthesis and surface engineering of iron oxide nanoparticles for biomedical applications. Biomaterials. 2005;26:3995–4021.
115. Xu C, Sun S. Monodisperse magnetic nanoparticles for biomedical applications. Polym Int. 2007;56:821–6.
116. Villanueva A, Cañete M, Roca AG, Calero M, Veintemillas-Verdaguer S, Serna CJ, del Puerto Morales M, Miranda R. The influence of surface functionalization on the enhanced internalization of magnetic nanoparticles in cancer cells. Nanotechnology. 2009;20:115103.
117. Arruebo M, Fernández-Pacheco R, Ibarra MR, Santamaría J. Magnetic nanoparticles for drug delivery. Nano Today. 2007;2:22–32.
118. Hugander A, Robins HI, Martin P, Schmitt C. Temperature distribution during radiant heat whole-body hyperthermia: experimental studies in the dog. Int J Hyperth. 1987;3:199–208.
119. Fortin J-P, Wilhelm C, Servais J, Ménager C, Bacri J-C, Gazeau F. Size-sorted anionic iron oxide nanomagnets as colloidal mediators for magnetic hyperthermia. J Am Chem Soc. 2007;129:2628–35.
120. Chung S, Hoffmann A, Bader S, Liu C, Kay B, Makowski L, Chen L. Biological sensors based on Brownian relaxation of magnetic nanoparticles. Appl Phys Lett. 2004;85:2971–3.
121. Kötitz R, Weitschies W, Trahms L, Brewer W, Semmler W. Determination of the binding reaction between avidin and biotin by relaxation measurements of magnetic nanoparticles. J Magn Magn Mater. 1999;194:62–8.

122. Soukup D, Moise S, Céspedes E, Dobson J, Telling ND. In situ measurement of magnetization relaxation of internalized nanoparticles in live cells. ACS Nano. 2015;9:231–40.
123. Dieckhoff J, Eberbeck D, Schilling M, Ludwig F. Magnetic-field dependence of Brownian and Néel relaxation times. J Appl Phys. 2016;119:043903.
124. Sharma P, Allison JP. Immune checkpoint targeting in cancer therapy: toward combination strategies with curative potential. Cell. 2015;161:205–14.
125. Wicki A, Witzigmann D, Balasubramanian V, Huwyler J. Nanomedicine in cancer therapy: challenges, opportunities, and clinical applications. J Control Release. 2015;200:138–57.
126. Qin S-Y, Zhang A-Q, Cheng S-X, Rong L, Zhang X-Z. Drug self-delivery systems for cancer therapy. Biomaterials. 2017;112:234–47.
127. Li S, Li C, Jin S, Liu J, Xue X, Eltahan AS, Sun J, Tan J, Dong J, Liang X-J. Overcoming resistance to cisplatin by inhibition of glutathione S-transferases (GSTs) with ethacraplatin micelles in vitro and in vivo. Biomaterials. 2017;144:119–29.
128. Espinosa A, Di Corato R, Kolosnjaj-Tabi J, Flaud P, Pellegrino T, Wilhelm C. Duality of iron oxide nanoparticles in cancer therapy: amplification of heating efficiency by magnetic hyperthermia and photothermal bimodal treatment. ACS Nano. 2016;10:2436–46.
129. Zhang Z, Wang J, Nie X, Wen T, Ji Y, Wu X, Zhao Y, Chen C. Near infrared laser-induced targeted cancer therapy using thermoresponsive polymer encapsulated gold nanorods. J Am Chem Soc. 2014;136:7317–26.
130. Singh A, Sahoo SK. Magnetic nanoparticles: a novel platform for cancer theranostics. Drug Discov Today. 2014;19:474–81.
131. Ling D, Lee N, Hyeon T. Chemical synthesis and assembly of uniformly sized iron oxide nanoparticles for medical applications. Acc Chem Res. 2015;48:1276–85.
132. Shi D, Sadat M, Dunn AW, Mast DB. Photo-fluorescent and magnetic properties of iron oxide nanoparticles for biomedical applications. Nanoscale. 2015;7:8209–32.
133. Zhou Q, Zhang B, Han D, Chen R, Qiu F, Wu J, Jiang H. Photo-responsive reversible assembly of gold nanoparticles coated with pillar [5] arenes. Chem Commun (Camb). 2015;51:3124–6.
134. Fantechi E, Innocenti C, Zanardelli M, Fittipaldi M, Falvo E, Carbo M, Shullani V, Di Cesare Mannelli L, Ghelardini C, Ferretti AM. A smart platform for hyperthermia application in cancer treatment: cobalt-doped ferrite nanoparticles mineralized in human ferritin cages. ACS Nano. 2014;8:4705–19.
135. Deatsch AE, Evans BA. Heating efficiency in magnetic nanoparticle hyperthermia. J Magn Magn Mater. 2014;354:163–72.
136. Pankhurst Q, Thanh N, Jones S, Dobson J. Progress in applications of magnetic nanoparticles in biomedicine. J Phys D Appl Phys. 2009;42:224001.
137. Hedayatnasab Z, Abnisa F, Daud WMAW. Review on magnetic nanoparticles for magnetic nanofluid hyperthermia application. Mater Des. 2017;123:174–96.
138. Conde J, Doria G, Baptista P. Noble metal nanoparticles applications in cancer. J Drug Deliv. 2012;2012:1.
139. Rosensweig RE. Heating magnetic fluid with alternating magnetic field. J Magn Magn Mater. 2002;252:370–4.
140. Garitaonandia JS, Insausti M, Goikolea E, Suzuki M, Cashion JD, Kawamura N, Ohsawa H, Gil de Muro I, Suzuki K, Plazaola F. Chemically induced permanent magnetism in Au, Ag, and Cu nanoparticles: iocalization of the magnetism by element selective techniques. Nano Lett. 2008;8:661–7.
141. Brezovich IA. Low frequency hyperthermia: capacitive and ferromagnetic thermoseed methods. Med Phys Mono. 1988;16:82–111.
142. Dennis C, Jackson A, Borchers J, Hoopes P, Strawbridge R, Foreman A, Van Lierop J, Grüttner C, Ivkov R. Nearly complete regression of tumors via collective behavior of magnetic nanoparticles in hyperthermia. Nanotechnology. 2009;20:395103.
143. Chatterjee J, Bettge M, Haik Y, Chen CJ. Synthesis and characterization of polymer encapsulated Cu–Ni magnetic nanoparticles for hyperthermia applications. J Magn Magn Mater. 2005;293:303–9.

144. Das R, Rinaldi-Montes N, Alonso J, Amghouz Z, Garaio E, García J, Gorria P, Blanco J, Phan M, Srikanth H. Boosted hyperthermia therapy by combined AC magnetic and photothermal exposures in Ag/Fe3O4 nanoflowers. ACS Appl Mater Interfaces. 2016;8:25162–9.
145. Jiang Q, Zheng S, Hong R, Deng S, Guo L, Hu R, Gao B, Huang M, Cheng L, Liu G. Folic acid-conjugated Fe3O4 magnetic nanoparticles for hyperthermia and MRI in vitro and in vivo. Appl Surf Sci. 2014;307:224–33.
146. Parchur AK, Sharma G, Jagtap JM, Gogineni VR, LaViolette PS, Flister MJ, White SB, Joshi A. Vascular interventional radiology-guided Photothermal therapy of colorectal Cancer liver metastasis with Theranostic gold Nanorods. ACS Nano. 2018;12:6597–611.
147. Han X, Huang J, Jing X, Yang D, Lin H, Wang Z, Li P, Chen Y. Oxygen-deficient Black Titania for synergistic/enhanced Sonodynamic and Photoinduced Cancer therapy at near infrared-II biowindow. ACS Nano. 2018;12:4545–55.
148. Saeed M, Iqbal MZ, Ren W, Xia Y, Liu C, Khan WS, Wu A. Controllable synthesis of Fe 3 O 4 nanoflowers: enhanced imaging guided cancer therapy and comparison of photothermal efficiency with black-TiO 2. J Mater Chem B. 2018;6:3800–10.
149. Gangopadhyay P, Gallet S, Franz E, Persoons A, Verbiest T. Novel superparamagnetic core (shell) nanoparticles for magnetic targeted drug delivery and hyperthermia treatment. IEEE Trans Magn. 2005;41:4194–6.
150. Martinez-Boubeta C, Simeonidis K, Serantes D, Conde-Leborán I, Kazakis I, Stefanou G, Peña L, Galceran R, Balcells L, Monty C. Adjustable hyperthermia response of self-assembled ferromagnetic Fe-MgO Core–Shell nanoparticles by tuning dipole–dipole interactions. Adv Funct Mater. 2012;22:3737–44.
151. Tian Q, Hu J, Zhu Y, Zou R, Chen Z, Yang S, Li R, Su Q, Han Y, Liu X. Sub-10 nm Fe_3O_4@ Cu_{2-x} S Core–Shell nanoparticles for dual-modal imaging and Photothermal therapy. J Am Chem Soc. 2013;135:8571–7.
152. Tang J, Zhou H, Liu J, Liu J, Li W, Wang Y, Hu F, Huo Q, Li J, Liu Y. Dual-mode imaging-guided synergistic chemo-and magnetohyperthermia therapy in a versatile nanoplatform to eliminate cancer stem cells. ACS Appl Mater Interfaces. 2017;9:23497–507.
153. Di Corato R, Béalle G, Kolosnjaj-Tabi J, Espinosa A, Clement O, Silva AK, Menager C, Wilhelm C. Combining magnetic hyperthermia and photodynamic therapy for tumor ablation with photoresponsive magnetic liposomes. ACS Nano. 2015;9:2904–16.
154. Berry CC, Curtis AS. Functionalisation of magnetic nanoparticles for applications in biomedicine. J Phys D Appl Phys. 2003;36:R198.
155. Guibert C, Dupuis V, Peyre V, Fresnais J. Hyperthermia of magnetic nanoparticles: experimental study of the role of aggregation. J Phys Chem C. 2015;119:28148–54.
156. Georgiadou V, Tangoulis V, Arvanitidis I, Kalogirou O, Dendrinou-Samara C. Unveiling the physicochemical features of CoFe2O4 nanoparticles synthesized via a variant hydrothermal method: NMR relaxometric properties. J Phys Chem C. 2015;119:8336–48.
157. Kotoulas A, Dendrinou-Samara C, Sarafidis C, Kehagias T, Arvanitidis J, Vourlias G, Angelakeris M, Kalogirou O. Carbon-encapsulated cobalt nanoparticles: synthesis, properties, and magnetic particle hyperthermia efficiency. J Nanopart Res. 2017;19:399.
158. Neuberger T, Schöpf B, Hofmann H, Hofmann M, Von Rechenberg B. Superparamagnetic nanoparticles for biomedical applications: possibilities and limitations of a new drug delivery system. J Magn Magn Mater. 2005;293:483–96.
159. Chen X, Klingeler R d, Kath M, El Gendy AA, Cendrowski K, Kalenczuk RJ, Borowiak-Palen E. Magnetic silica nanotubes: synthesis, drug release, and feasibility for magnetic hyperthermia. ACS Appl Mater Interfaces. 2012;4:2303–9.
160. Beg S, Rizwan M, Sheikh AM, Hasnain MS, Anwer K, Kohli K. Advancement in carbon nanotubes: basics, biomedical applications and toxicity. J Pharm Pharmacol. 2011;63:141–63.
161. Zuo X, Wu C, Zhang W, Gao W. Magnetic carbon nanotubes for self-regulating temperature hyperthermia. RSC Adv. 2018;8:11997–2003.
162. Widder KJ, Senyei AE, Scarpelli DG. Magnetic microspheres: a model system for site specific drug delivery in vivo. Proc Soc Exp Biol Med. 1978;158:141–6.

163. Zhe Liu FK, Gätjens J. Advanced nanomaterials in multimodal imaging: design, functionalization, and biomedical applications. J Nanomater. 2010;2010:15.
164. Obeid MA, Al Qaraghuli MM, Alsaadi M, Alzahrani AR, Niwasabutra K, Ferro VA. Delivering natural products and biotherapeutics to improve drug efficacy. Ther Deliv. 2017;8:947–56.
165. Miele E, Spinelli GP, Miele E, Di Fabrizio E, Ferretti E, Tomao S, Gulino A. Nanoparticle-based delivery of small interfering RNA: challenges for cancer therapy. Int J Nanomedicine. 2012;7:3637.
166. Saadeh Y, Vyas D. Nanorobotic applications in medicine: current proposals and designs. Am J Robot Surg. 2014;1:4–11.
167. Holzinger M, Le Goff A, Cosnier S. Nanomaterials for biosensing applications: a review. Front Chem. 2014;2:63.
168. De Jong WH, Borm PJ. Drug delivery and nanoparticles: applications and hazards. Int J Nanomedicine. 2008;3:133.
169. Almalik A, Benabdelkamel H, Masood A, Alanazi IO, Alradwan I, Majrashi MA, Alfadda AA, Alghamdi WM, Alrabiah H, Tirelli N. Hyaluronic acid coated chitosan nanoparticles reduced the immunogenicity of the formed protein Corona. Sci Rep. 2017;7:10542.
170. Martens TF, Remaut K, Deschout H, Engbersen JF, Hennink WE, Van Steenbergen MJ, Demeester J, De Smedt SC, Braeckmans K. Coating nanocarriers with hyaluronic acid facilitates intravitreal drug delivery for retinal gene therapy. J Control Release. 2015;202:83–92.
171. Kolhar P, Anselmo AC, Gupta V, Pant K, Prabhakarpandian B, Ruoslahti E, Mitragotri S. Using shape effects to target antibody-coated nanoparticles to lung and brain endothelium. Proc Natl Acad Sci. 2013;110:10753–8.
172. Müller J, Bauer KN, Prozeller D, Simon J, Mailänder V, Wurm FR, Winzen S, Landfester K. Coating nanoparticles with tunable surfactants facilitates control over the protein corona. Biomaterials. 2017;115:1–8.
173. Gao W, Zhang L. Coating nanoparticles with cell membranes for targeted drug delivery. J Drug Target. 2015;23:619–26.
174. Gao H, Yang Z, Zhang S, Cao S, Shen S, Pang Z, Jiang X. Ligand modified nanoparticles increases cell uptake, alters endocytosis and elevates glioma distribution and internalization. Sci Rep. 2013;3:2534.
175. Lu H, Wang J, Wang T, Zhong J, Bao Y, Hao H. Recent progress on nanostructures for drug delivery applications. J Nanomater. 2016;2016:20.
176. Kumari A, Kumar V, Yadav S. Nanotechnology: a tool to enhance therapeutic values of natural plant products. Trends Med Res. 2012;7:34–42.
177. Patra JK, Das G, Fraceto LF, Campos EVR, del Pilar Rodriguez-Torres M, Acosta-Torres LS, Diaz-Torres LA, Grillo R, Swamy MK, Sharma S. Nano based drug delivery systems: recent developments and future prospects. J Nanobiotechnol. 2018;16:71.
178. Xu L, Qiu L, Sheng Y, Sun Y, Deng L, Li X, Bradley M, Zhang R. Biodegradable pH-responsive hydrogels for controlled dual-drug release. J Mater Chem B. 2018;6:510–7.
179. Al-Ahmady Z, Kostarelos K. Chemical components for the design of temperature-responsive vesicles as cancer therapeutics. Chem Rev. 2016;116:3883–918.
180. Zhang Z, Zhang D, Wei L, Wang X, Xu Y, Li H-W, Ma M, Chen B, Xiao L. Temperature responsive fluorescent polymer nanoparticles (TRFNPs) for cellular imaging and controlled releasing of drug to living cells. Colloids Surf B: Biointerfaces. 2017;159:905–12.
181. Bai Y, Xie F-Y, Tian W. Controlled self-assembly of Thermo-responsive amphiphilic H-shaped polymer for adjustable drug release. Chin J Polym Sci. 2018;36:406–16.
182. Anirudhan T, Nair AS. Temperature and ultrasound sensitive gatekeepers for the controlled release of chemotherapeutic drugs from mesoporous silica nanoparticles. J Mater Chem B. 2018;6:428–39.
183. Mathiyazhakan M, Wiraja C, Xu C. A concise review of gold nanoparticles-based photo-responsive liposomes for controlled drug delivery. Nano-Micro Lett. 2018;10:10.

184. Hervault A, Thanh NTK. Magnetic nanoparticle-based therapeutic agents for thermo-chemotherapy treatment of cancer. Nanoscale. 2014;6:11553–73.
185. Guo Y, Zhang Y, Ma J, Li Q, Li Y, Zhou X, Zhao D, Song H, Chen Q, Zhu X. Light/magnetic hyperthermia triggered drug released from multi-functional thermo-sensitive magnetoliposomes for precise cancer synergetic theranostics. J Control Release. 2018;272:145–58.
186. Ma G, Lin W, Yuan Z, Wu J, Qian H, Xu L, Chen S. Development of ionic strength/pH/enzyme triple-responsive zwitterionic hydrogel of the mixed L-glutamic acid and L-lysine polypeptide for site-specific drug delivery. J Mater Chem B. 2017;5:935–43.
187. Alonso J, Khurshid H, Devkota J, Nemati Z, Khadka NK, Srikanth H, Pan J, Phan M-H. Superparamagnetic nanoparticles encapsulated in lipid vesicles for advanced magnetic hyperthermia and biodetection. J Appl Phys. 2016;119:083904.
188. Grillo R, Gallo J, Stroppa DG, Carbó-Argibay E, Lima R, Fraceto LF, Bañobre-López M. Sub-micrometer magnetic nanocomposites: insights into the effect of magnetic nanoparticles interactions on the optimization of SAR and MRI performance. ACS Appl Mater Interfaces. 2016;8:25777–87.
189. Ulbrich K, Hola K, Subr V, Bakandritsos A, Tucek J, Zboril R. Targeted drug delivery with polymers and magnetic nanoparticles: covalent and noncovalent approaches, release control, and clinical studies. Chem Rev. 2016;116:5338–431.
190. Chen C-W, Syu W-J, Huang T-C, Lee Y-C, Hsiao J-K, Huang K-Y, Yu H-P, Liao M-Y, Lai P-S. Encapsulation of au/Fe 3 O 4 nanoparticles into a polymer nanoarchitecture with combined near infrared-triggered chemo-photothermal therapy based on intracellular secondary protein understanding. J Mater Chem B. 2017;5:5774–82.
191. Wu W, Jiang CZ, Roy VA. Designed synthesis and surface engineering strategies of magnetic iron oxide nanoparticles for biomedical applications. Nanoscale. 2016;8:19421–74.
192. Wahajuddin SA. Superparamagnetic iron oxide nanoparticles: magnetic nanoplatforms as drug carriers. Int J Nanomedicine. 2012;7:3445.
193. Prijic S, Sersa G. Magnetic nanoparticles as targeted delivery systems in oncology. Radiol Oncol. 2011;45:1–16.
194. El-Boubbou K. Magnetic iron oxide nanoparticles as drug carriers: clinical relevance. Nanomedicine. 2018;13:953–71.
195. Laurent S, Saei AA, Behzadi S, Panahifar A, Mahmoudi M. Superparamagnetic iron oxide nanoparticles for delivery of therapeutic agents: opportunities and challenges. Expert Opin Drug Deliv. 2014;11:1449–70.
196. Gao Z, Li Y, You C, Sun K, An P, Sun C, Wang M, Zhu X, Sun B. Iron oxide nanocarrier-mediated combination therapy of cisplatin and artemisinin for combating drug resistance through highly increased toxic reactive oxygen species generation. ACS Appl Bio Mater. 2018;1:270–80.
197. Kosmas C, Muñoz Estrella A, Sourlas A, Silverio D, Hilario E, Montan P, Guzman E. Inclisiran: a new promising agent in the management of hypercholesterolemia. Diseases. 2018;6:63.
198. Prilepskii AY, Fakhardo AF, Drozdov AS, Vinogradov VV, Dudanov IP, Shtil AA, Bel'tyukov PP, Shibeko AM, Koltsova EM, Nechipurenko DY. Urokinase-conjugated magnetite nanoparticles as a promising drug delivery system for targeted thrombolysis: synthesis and preclinical evaluation. ACS Appl Mater Interfaces. 2018;10:36764–75.
199. Hsiao M-H, Mu Q, Stephen ZR, Fang C, Zhang M. Hexanoyl-chitosan-PEG copolymer coated iron oxide nanoparticles for hydrophobic drug delivery. ACS Macro Lett. 2015;4:403–7.
200. Clary L, Verderone G, Santaella C, Vierling P. Membrane permeability and stability of liposomes made from highly fluorinated double-chain phosphocholines derived from diaminopropanol, serine or ethanolamine. Biochim Biophys Acta Biomembr. 1997;1328:55–64.
201. Gabizon A, Dagan A, Goren D, Barenholz Y, Fuks Z. Liposomes as in vivo carriers of adriamycin: reduced cardiac uptake and preserved antitumor activity in mice. Cancer Res. 1982;42:4734–9.

202. Immordino ML, Brusa P, Arpicco S, Stella B, Dosio F, Cattel L. Preparation, characterization, cytotoxicity and pharmacokinetics of liposomes containing docetaxel. J Control Release. 2003;91:417–29.
203. Zhao Y, Zhao X, Cheng Y, Guo X, Yuan W. Iron oxide nanoparticles-based vaccine delivery for Cancer treatment. Mol Pharm. 1791-1799;2018:15.
204. Mody KT, Popat A, Mahony D, Cavallaro AS, Yu C, Mitter N. Mesoporous silica nanoparticles as antigen carriers and adjuvants for vaccine delivery. Nanoscale. 2013;5:5167–79.
205. Gillies RJ, Bhujwalla ZM, Evelhoch J, Garwood M, Neeman M, Robinson SP, Sotak CH, Van Der Sanden B. Applications of magnetic resonance in model systems: tumor biology and physiology. Neoplasia (New York, NY). 2000;2:139–51.
206. Furman-Haran E, Schechtman E, Kelcz F, Kirshenbaum K, Degani H. Magnetic resonance imaging reveals functional diversity of the vasculature in benign and malignant breast lesions. Cancer. 2005;104:708–18.
207. Bowtell R. Colourful future for MRI. Nature. 2008;453:993.
208. Mornet S, Vasseur S, Grasset F, Veverka P, Goglio G, Demourgues A, Portier J, Pollert E, Duguet E. Magnetic nanoparticle design for medical applications. Prog Solid State Chem. 2006;34:237–47.
209. Hoehn M, Himmelreich U, Kruttwig K, Wiedermann D. Molecular and cellular MR imaging: potentials and challenges for neurological applications. J Magn Reson Imaging. 2008;27:941–54.
210. Alford R, Ogawa M, Choyke PL, Kobayashi H. Molecular probes for the in vivo imaging of cancer. Mol Bio Syst. 2009;5:1279–91.
211. Longmire M, Choyke PL, Kobayashi H. Dendrimer-based contrast agents for molecular imaging. Curr Top Med Chem. 2008;8:1180–6.
212. Bouzigues C, Gacoin T, Alexandrou A. Biological applications of rare-earth based nanoparticles. ACS Nano. 2011;5:8488–505.
213. Hanaoka K. Development of responsive lanthanide-based magnetic resonance imaging and luminescent probes for biological applications. Chem Pharm Bull. 2010;58:1283–94.
214. Na HB, Song IC, Hyeon T. Inorganic nanoparticles for MRI contrast agents. Adv Mater. 2009;21:2133–48.
215. Ivanuša T, Beravs K, Medič J, Serša I, Serša G, Jevtič V, Demsar F, Mikac U. Dynamic contrast enhanced MRI of mouse fibrosarcoma using small-molecular and novel macromolecular contrast agents. Phys Med. 2007;23:85–90.
216. Terreno E, Castelli DD, Viale A, Aime S. Challenges for molecular magnetic resonance imaging. Chem Rev. 2010;110:3019–42.
217. Ripoll J, Ntziachristos V, Cannet C, Babin AL, Kneuer R, Gremlich H-U, Beckmann N. Investigating pharmacology in vivo using magnetic resonance and optical imaging. Drugs RD. 2008;9:277–306.
218. Reilly RF. Risk for nephrogenic systemic fibrosis with gadoteridol (pro Hance) in patients who are on long-term hemodialysis. Clin J Am Soc Nephrol CJASN. 2008;3:747–51.
219. Reiter T, Ritter O, Prince MR, Nordbeck P, Wanner C, Nagel E, Bauer WR. Minimizing risk of nephrogenic systemic fibrosis in cardiovascular magnetic resonance. J Cardiovasc Magn Reson. 2012;14:31.
220. McCarthy JR, Weissleder R. Multifunctional magnetic nanoparticles for targeted imaging and therapy. Adv Drug Deliv Rev. 2008;60:1241–51.
221. Lawaczeck R, Menzel M, Pietsch H. Superparamagnetic iron oxide particles: contrast media for magnetic resonance imaging. Appl Organomet Chem. 2004;18:506–13.
222. Hu S-H, Gao X. Nanocomposites with spatially separated functionalities for combined imaging and Magnetolytic therapy. J Am Chem Soc. 2010;132:7234–7.
223. Jun Y-w, Choi J-s, Cheon J. Heterostructured magnetic nanoparticles: their versatility and high performance capabilities. Chem Commun. 2007:1203–14.

224. Fulton DA, O'Halloran M, Parker D, Senanayake K, Botta M, Aime S. Efficient relaxivity enhancement in dendritic gadolinium complexes: effective motional coupling in medium molecular weight conjugates. Chem Commun. 2005:474–6.
225. Haris M, Yadav SK, Rizwan A, Singh A, Wang E, Hariharan H, Reddy R, Marincola FM. Molecular magnetic resonance imaging in cancer. J Transl Med. 2015;13:313.
226. Singh N, Jenkins GJS, Asadi R, Doak SH. Potential toxicity of superparamagnetic iron oxide nanoparticles (SPION). Nano Rev. 2010;1 https://doi.org/10.3402/nano.v3401i3400.5358.
227. Veiseh O, Gunn JW, Zhang M. Design and fabrication of magnetic nanoparticles for targeted drug delivery and imaging. Adv Drug Deliv Rev. 2010;62:284–304.
228. Lin MM, Kim DK, Haj AJE, Dobson J. Development of Superparamagnetic Iron Oxide Nanoparticles (SPIONS) for translation to clinical applications. IEEE Trans Nano Biosci. 2008;7:298–305.
229. Nathan J, Wittenberg CLH. Using nanoparticles to push the limits of detection. Wiley Interdiscip Rev Nanomed Nanobiotechnol. 2009;1:237–54.